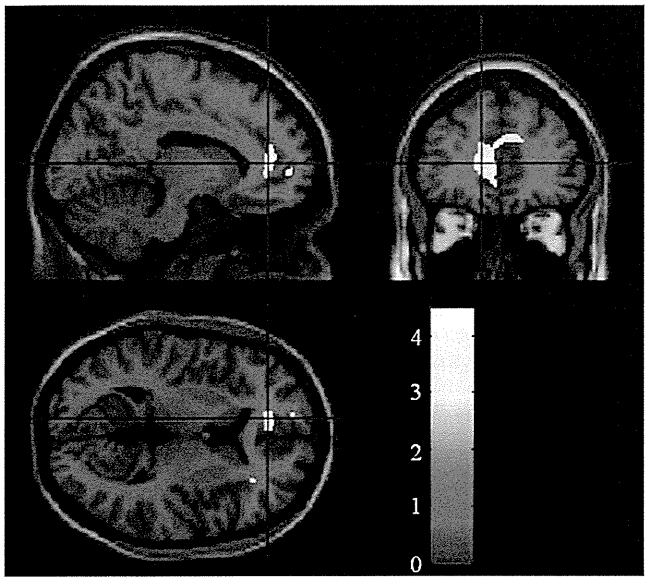

FIGURE 1 | Group difference of the gray matter between the schizophrenia patients and the healthy controls. The cluster in which the schizophrenia patients show gray matter reduction is located in the left anterior cingulate gyrus.

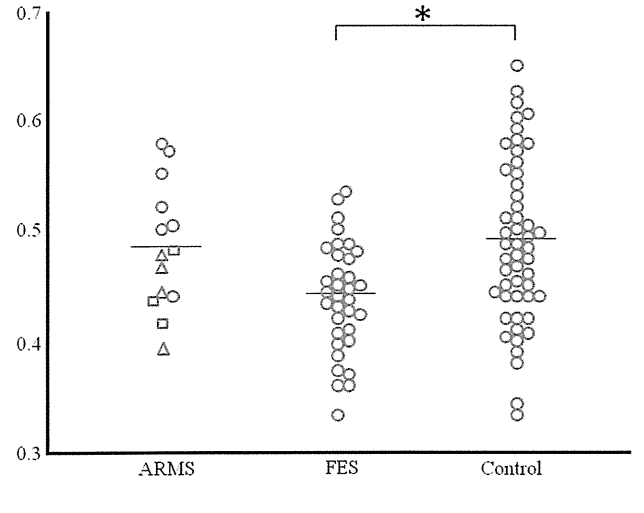

FIGURE 2 | Scatter plots of gray matter volume of the peak coordinate at the left anterior cingulate gyrus that revealed the difference between schizophrenia patients and controls. The ARMS subjects were classified into three groups according to clinical outcome (square: ARMS who developed psychosis, triangle: ARMS with unknown outcome, circle: ARMS without transition to psychosis). *$p < 0.05$.

cingulate gyrus have been revealed by MRI studies in first-episode and neuroleptic-naïve patients to minimize the influence of neuroleptic medication or chronicity of the illness. In this study, gray matter volume reduction in the left anterior cingulate gyrus in the schizophrenia patients had no relationship with any effects of medication (data not shown).

Table 2 | Talairach coordinates for regions of reduced gray matter volume in the schizophrenia patients compared to the healthy controls.

Region	Voxel	Peak coordinate			*T*	*p*
		x	*y*	*z*		
lt. anterior cingulate gyrus	631	−11	42	8	3.82	0.047

One major aim of high-risk studies for psychosis has been to identify clinical and neurobiological predictors of future transition to psychosis, which would allow specific and targeted preventive strategies (McGorry et al., 2006); indeed, previous neuroimaging studies have identified such predictive markers. The VBM study by Pantelis et al. (2003) revealed the association between later transition and gray matter reduction in temporal and frontal regions predominantly in the right hemisphere and cingulate gyrus bilaterally in clinical high-risk subjects, which was largely replicated in an independent high-risk cohort (Borgwardt et al., 2007). Recent multi-center (Mechelli et al., 2011) and meta-analytic (Smieskova et al., 2010; Fusar-Poli et al., 2011) MRI studies on large numbers of high-risk subjects generally supported the assertion that brain morphological changes in the fronto-temporo-limbic regions, including the cingulate gyrus, already exist prior to the onset of psychosis. Although our data are clearly limited by the small sample size as discussed below, the distribution of the anterior cingulate gray matter volume (**Figure 2**) implies that ARMS subjects with later transition may have morphological changes of the cingulate gyrus to the same degree as those with overt schizophrenia. There has been debate about the risk-benefit ratio of antipsychotic treatment in prodromal patients (Woods et al., 2007; Weiser, 2011). However, given the hypothesized active brain pathology in the early phases of psychosis, which could affect the subsequent course of the illness (Birchwood et al., 1998), and the potential ameliorating effects of atypical antipsychotics for brain structural abnormalities (Lieberman et al., 2005; Girgis et al., 2006), intervention before the expression of frank psychosis may reduce neurobiological deterioration as well as the transition rate to psychosis (McGorry et al., 2002; McGlashan et al., 2006), especially in subjects with neurobiological risk markers.

The sample size of the current ARMS group (especially those who later developed psychosis) was small and some individuals dropped out during clinical follow-up ($N = 4$, unknown outcome group). Significant group differences in age (ARMS < schizophrenia and controls) might also have biased our results, although we used age as a controlling factor in all imaging analyses. In contrast to our prediction, we did not find significant brain morphological changes in the ARMS subjects, potentially due to the small sample size. It was also not possible to examine the relationship between brain morphology and clinical outcome (later transition) in our ARMS subjects statistically. In addition, direct comparison between the three groups using the ANOVA model with age and ICV as covariates failed to replicate significant group difference in the cingulate gyrus gray matter volume. Thus, further study with a larger well-defined

sample is required to replicate and expand the current preliminary results.

In summary, the present study demonstrated significant gray matter reduction of the anterior cingulate gyrus in first-episode schizophrenia. We also suggested the possibility that such morphological change may exist prior to the onset of psychosis in some individuals, implying the potential role of neuroimaging methods in the prediction of future transition and effective intervention for high-risk subjects.

ACKNOWLEDGMENTS

This research was supported in part by Grants-in-Aid for Scientific Research (C) (No. 22591275, 24591699) and Grants-in-Aid for Scientific Research (B) (No. 24390281) from the Japanese Society for the Promotion of Science, Health and Labour Sciences Research Grants (Comprehensive Research on Disability, Health and Welfare, H23-Seishin-Ippan-002 and H23-Seishin-Ippan-009), and a Research Grant from the JSPS Asian Core Program.

REFERENCES

Andreasen, N. C. (1983). *The Scale for the Assessment of Negative Symptoms (SANS).* Iowa City: University of Iowa.

Andreasen, N. C. (1984). *The Scale for the Assessment of Positive Symptoms (SAPS).* Iowa City: University of Iowa.

Andreasen, N. C., Flaum, M., and Arndt, S. (1992). The comprehensive assessment of symptoms and history (CASH): an instrument for assessing diagnosis and psychopathology. *Arch. Gen. Psychiatry* 49, 615–623.

Andreasen, N. C., Nopoulos, P., Magnotta, V., Pierson, R., Ziebell, S., and Ho, B. C. (2011). Progressive brain change in schizophrenia: a prospective longitudinal study of first-episode schizophrenia. *Biol. Psychiatry* 70, 672–679.

Ashburner, J. (2007). A fast diffeomorphic image registration algorithm. *Neuroimage* 38, 95–113.

Ashburner, J., and Friston, K. J. (2005). Unified segmentation. *Neuroimage* 26, 839–851.

Ashburner, J., and Friston, K. J. (2009). Computing average shaped tissue probability templates. *Neuroimage* 45, 333–341.

Birchwood, M., Todd, P., and Jackson, C. (1998). Early intervention in psychosis: the critical-period hypothesis. *Br. J. Psychiatry Suppl.* 172, 53–59.

Borgwardt, S. J., Riecher-Rössler, A., Dazzan, P., Chitnis, X., Aston, J., Drewe, M., et al. (2007). Regional gray matter volume abnormalities in the at risk mental state. *Biol. Psychiatry* 61, 1148–1156.

Ellison-Wright, I., Glahn, D. C., Laird, A. R., Thelen, S. M., and Bullmore, E. (2008). The anatomy of first-episode and chronic schizophrenia: an anatomical likelihood estimation meta-analysis. *Am. J. Psychiatry* 165, 1015–1023.

Fornito, A., Yung, A. R., Wood, S. J., Phillips, L. J., Nelson, B., Cotton, S., et al. (2008). Anatomic abnormalities of the anterior cingulate cortex before psychosis onset: an MRI study of ultra-high-risk individuals. *Biol. Psychiatry* 64, 758–765.

Fusar-Poli, P., Bonoldi, I., Yung, A. R., Borgwardt, S., Kempton, M. J., Valmaggia, L., et al. (2012). Predicting psychosis, meta-analysis of transition outcomes in individuals at high clinical risk. *Arch. Gen. Psychiatry* 69, 220–229.

Fusar-Poli, P., Borgwardt, S., Crescini, A., Deste, G., Kempton, M. J., Lawrie, S., et al. (2011). Neuroanatomy of vulnerability to psychosis: a voxel-based meta-analysis. *Neurosci. Biobehav. Rev.* 35, 1175–1185.

Gaser, C. (2009). *Voxel-Based Morphometry Toolbox, Version 8 (vbm8).* Available at: http://dbm.neuro.uni-jena.de

Girgis, R. R., Diwadkar, V. A., Nutche, J. J., Sweeney, J. A., Keshavan, M. S., and Hardan, A. Y. (2006). Risperidone in first-episode psychosis: a longitudinal, exploratory voxel-based morphometric study. *Schizophr. Res.* 82, 89–94.

Hayasaka, S., Phan, K. L., Liberzon, I., Worsley, K. J., and Nichols, T. E. (2004). Nonstationary cluster-size inference with random field and permutation methods. *Neuroimage* 22, 676–687.

Jones, D. K., Symms, M. R., Cercignani, M., and Howard, R. J. (2005). The effect of filter size on VBM analyses of DT-MRI data. *Neuroimage* 26, 546–554.

Klein, A., Anderson, J., Ardekani, B. A., Ashburner, J., Avants, B., Chiang, M. C., et al. (2009). Evaluation of 14 nonlinear deformation algorithms applied to human brain MRI registration. *Neuroimage* 46, 786–802.

Koo, M. S., Levitt, J. L., Salisbury, D. F., Nakamura, M., Shenton, M. E., and McCarley, R. W. (2008). A cross-sectional and longitudinal magnetic resonance imaging study of cingulate gyrus gray matter volume abnormalities in first-episode schizophrenia and first-episode affective psychosis. *Arch. Gen. Psychiatry* 65, 746–760.

Lappin, J. M., Morgen, K., Morgen, C., Hutchison, G., Chitnis, X., Sucking, J., et al. (2006). Gray matter abnormalities associated with duration of untreated psychosis. *Schizophr. Res.* 83, 145–153.

Leung, M., Cheung, C., Yu, K., Yip, B., Sham, P., Li, Q., et al. (2011). Gray matter in first-episode schizophrenia before and after antipsychotic drug treatment. Anatomical likelihood estimation meta-analyses with sample size weighting. *Schizophr. Bull.* 37, 199–211.

Lieberman, J. A., Tollefson, G. D., Charles, C., Zipursky, R., Sharma, T., Kahn, R. S., et al. (2005). Antipsychotic drug effects on brain morphology in first-episode schizophrenia. *Arch. Gen. Psychiatry* 62, 361–370.

Marshall, M., Lewis, S., Lockwood, A., Drake, R., Jones, P., and Croudace, T. (2005). Association between duration of untreated psychosis and outcome in cohorts of first-episode patients: a systematic review. *Arch. Gen. Psychiatry* 62, 975–983.

McGlashan, T. H., Zipursky, R. B., Perkins, D., Addington, J., Miller, T., Woods, S. W., et al. (2006). Randomized, double-blind trial of olanzapine versus placebo in patients prodromally symptomatic for psychosis. *Am. J. Psychiatry* 163, 790–799.

McGorry, P. D., Hickie, I. B., Yung, A. R., Pantelis, C., and Jackson, H. J. (2006). Clinical staging of psychiatric disorders: a heuristic framework for choosing earlier, safer and more effective interventions. *Aust. N. Z. J. Psychiatry* 40, 616–622.

McGorry, P. D., Yung, A. R., Phillips, L. J., Yuen, H. P., Francey, S., Cosgrave, E. M., et al. (2002). Randomized controlled trial of interventions designed to reduce the risk of progression to first-episode psychosis in a clinical sample with subthreshold symptoms. *Arch. Gen. Psychiatry* 59, 921–928.

Mechelli, A., Riecher-Rössler, A., Meisenzahl, E. M., Tognin, S., Wood, S. J., Borgwardt, S. J., et al. (2011). Neuroanatomical abnormalities that predate the onset of psychosis: a multicenter study. *Arch. Gen. Psychiatry* 68, 489–495.

Meisenzahl, E. M., Koutsouleris, N., Gaser, C., Bottelender, R., Schmitt, G. J. E., McGuire, P., et al. (2008). Structural brain alterations in subjects at high-risk of psychosis: a voxel-based morphometric study. *Schizophr. Res.* 102, 150–162.

Mizuno, M., Suzuki, M., Matsumoto, K., Murakami, M., Takeshi, K., Miyakoshi, T., et al. (2009). Clinical practice and research activities for early psychiatric intervention at Japanese leading centres. *Early Interv. Psychiatry* 3, 5–9.

Pantelis, C., Velakoulis, D., McGorry, P. D., Wood, S. J., Suckling, J., Phillips, L. J., et al. (2003). Neuroanatomical abnormalities before and after onset of psychosis: a cross-sectional and longitudinal MRI comparison. *Lancet* 361, 281–288.

Perkins, D. O., Gu, H., Boteva, K., and Lieberman, J. A. (2005). Relationship between duration of untreated psychosis and outcome in first-episode schizophrenia: a critical review and meta-analysis. *Am. J. Psychiatry* 162, 1785–1804.

Salgado-Pineda, P., Baeza, I., Pérez-Gómez, M., Vendrell, P., Junqué, C., Bargalló, N., et al. (2003). Sustained attention impairment correlates to gray matter decreases in first episode neuroleptic-naive schizophrenic patients. *Neuroimage* 19, 365–375.

Salmond, C. H., Asburner, J., Vargha-Khadem, F., Connelly, A., Gadian, D. G., and Fristion, K. J. (2002). Distributional assumptions in voxel-based morphometry. *Neuroimage* 17, 1027–1030.

Schultz, C. C., Koch, K., Wagner, G., Roebel, M., Schachtzabel, C., Gaser, C., et al. (2010). Reduced cortical thickness in first episode schizophrenia. *Schizophr. Res.* 116, 204–209.

Shepherd, A. M., Laurens, K. R., Matheson, S. L., Carr, S. M., and Green, M. J. (2012). Systematic meta-review and quality assessment of the structural brain alterations in schizophrenia. *Neurosci. Biobehav. Rev.* 36, 1342–1356.

Smieskova, R., Fusar-Poli, P., Allen, P., Bendfeldt, K., Stieglitz, R. D., Drewe, J., et al. (2010). Neuroimaging predictors of transition to psychosis–a systematic review and meta-analysis. *Neurosci. Biobehav. Rev.* 34, 1207–1222.

Steen, R. G., Mull, C., McClure, R., Hamer, R. M., and Lieberman, J. A. (2006). Brain volume in first episode schizophrenia: systematic review and meta-analysis of magnetic resonance imaging studies. *Br. J. Psychiatry* 188, 510–518.

Takahashi, T., Suzuki, M., Tanino, R., Zhou, S.-Y., Hagino, H., Niu, L., et al. (2007). Volume reduction of the left planum temporal gray matter associated with long duration of untreated psychosis in schizophrenia: preliminary report. *Psychiatry Res.* 154, 209–219.

Takahashi, T., Suzuki, M., Zhou, S.-Y., Tanino, R., Nakamura, K., Kawasaki, Y., et al. (2010). A follow-up MRI study of the superior temporal subregions in schizotypal disorder and first-episode schizophrenia. *Schizophr. Res.* 119, 65–74.

Takahashi, T., Zhou, S.-Y., Nakamura, K., Tanino, R., Furuichi, A., Kido, M., et al. (2011). A follow-up MRI study of the fusiform gyrus and middle and inferior temporal gyri in schizophrenia spectrum. *Prog. Neuropsychopharmacol. Biol. Psychiatry* 35, 1957–1964.

Talairach, J., and Tournoux, P. (1988). *Co-Planar Stereotaxic Atlas of the Human Brain.* New York: Thieme Medical Publishers.

Toru, M. (2001). *Psychotropic Manual,* 2nd Edn. Tokyo: Igaku-Shoin. (in Japanese).

Vita, A., De Peri, L., Silenzi, C., and Dicci, M. (2006). Brain morphology in first-episode schizophrenia: a meta-analysis of quantitative magnetic resonance imaging studies. *Schizophr. Res.* 82, 75–88.

Weiser, M. (2011). Early intervention for schizophrenia: the risk-benefit ratio of antipsychotic treatment in the prodromal phase. *Am. J. Psychiatry* 168, 761–763.

Woods, S. W., Tully, E. M., Walsh, B. C., Hawkins, K. A., Callahan, J. L., Cohen, S. J., et al. (2007). Aripiprazole in the treatment of the psychosis prodrome: an open-label pilot study. *Br. J. Psychiatry* 191, 96–101.

World Health Organization. (1993). *The ICD-10 Classification of Mental and Behavioural Disorders: Diagnostic Criteria for Research.* Geneva: World Health Organization.

Worsley, K. J., Andermann, M., Koulis, T., MacDonald, D., and Evans, A. C. (1999). Detecting changes in nonisotropic images. *Hum. Brain Mapp.* 8, 98–101.

Yung, A. R., Phillips, L. J., and McGorry, P. D. (2004). *Treating Schizophrenia in the Prodromal Phase.* London: Taylor & Francis.

Yung, A. R., Phillips, L. J., Yuen, H. P., Francey, S. M., McFarlane, C. A., Hallgren, M., et al. (2003). Psychosis prediction: 12-month follow up of a high-risk ("prodromal") group. *Schizophr. Res.* 60, 21–32.

Conflict of Interest Statement: The authors declare that the research was conducted in the absence of any commercial or financial relationships that could be construed as a potential conflict of interest.

Received: 26 December 2012; accepted: 01 March 2013; published online: 18 March 2013.

Citation: Nakamura K, Takahashi T, Nemoto K, Furuichi A, Nishiyama S, Nakamura Y, Ikeda E, Kido M, Noguchi K, Seto H and Suzuki M (2013) Gray matter changes in subjects at high risk for developing psychosis and first-episode schizophrenia: a voxel-based structural MRI study. Front. Psychiatry **4**:16. doi: 10.3389/fpsyt.2013.00016*

This article was submitted to Frontiers in Schizophrenia, a specialty of Frontiers in Psychiatry.

ORIGINAL RESEARCH

Automatic Voxel-Based Morphometry of Structural MRI by SPM8 plus Diffeomorphic Anatomic Registration Through Exponentiated Lie Algebra Improves the Diagnosis of Probable Alzheimer Disease

H. Matsuda
S. Mizumura
K. Nemoto
F. Yamashita
E. Imabayashi
N. Sato
T. Asada


BACKGROUND AND PURPOSE: The necessity for structural MRI is greater than ever to both diagnose AD in its early stage and objectively evaluate its progression. We propose a new VBM-based software program for automatic detection of early specific atrophy in AD.

MATERIALS AND METHODS: A target VOI was determined by group comparison of 30 patients with very mild AD and 40 age-matched healthy controls by using SPM. Then this target VOI was incorporated into a newly developed automated software program independently running on a Windows PC for VBM by using SPM8 plus DARTEL. ROC analysis was performed for discrimination of 116 other patients with AD with very mild stage (n = 45), mild stage (n = 30) and moderate-to-advanced stages (n = 41) from 40 other age-matched healthy controls by using a z score map in the target VOI.

RESULTS: Medial temporal structures involving the entire region of the entorhinal cortex, hippocampus, and amygdala showed significant atrophy in the patients with very mild AD and were determined as a target VOI. When we used the severity score of atrophy in this target VOI, 91.6%, 95.8%, and 98.2% accuracies were obtained in the very mild AD, mild AD, and moderate-to-severe AD groups, respectively. In the very mild AD group, a high specificity of 97.5% with a sensitivity of 86.4% was obtained, and age at onset of AD did not influence this accuracy.

CONCLUSIONS: This software program with application of SPM8 plus DARTEL to VBM provides a high performance for AD diagnosis by using MRI.

ABBREVIATIONS: AD = Alzheimer disease; DARTEL = diffeomorphic anatomical registration through exponentiated lie algebra; FWHM = full width at half maximum; MCI = mild cognitive impairment; MMSE = Mini-Mental State Examination; ROC = receiver operating characteristic analysis; SPM = statistical parametric mapping; VBM = voxel-based morphometry

Increases in the number of individuals with dementia, the highest proportion of whom are affected by AD, have made early diagnosis of AD a major research and clinical priority. Of several neuroimaging techniques that provide surrogate markers for the diagnosis of AD, structural MRI is the most commonly used because of its noninvasiveness and excellent spatial resolution with good tissue contrast.[1] In AD, the earliest tissue loss occurs in the medial temporal structures, particularly in the entorhinal cortex.[2] However, visual inspection is insufficient for objective evaluation of mild atrophy. Although manual tracing of these structures can quantify the absolute volume, it is time-consuming and requires special expertise in anatomic knowledge for tracers. Recently, computer-aided VBM[3] has been applied to detect early atrophic changes in AD. Although this technique cannot provide the absolute volume, it can provide statistical results in comparisons of patients with AD with healthy controls.[4] Moreover VBM has been reported to be a surrogate indicator of the full brain topographic representation of the neurodegenerative aspect of AD pathology.[5] Hirata et al[6] proposed an automated software program, a voxel-based specific regional analysis system for AD, for the diagnosis of AD by using this VBM technique. In the present study, we revised this software by introducing new techniques and validated its utility.

Materials and Methods

A total of 251 subjects were studied in 1 center. We retrospectively chose 146 patients (65 men and 81 women) with a clinical diagnosis of probable AD according to the National Institute of Neurologic and Communicative Disorders and Stroke and the Alzheimer Disease and Related Disorders Association criteria.[7] These patients were classified into 3 groups of very mild, mild, and moderate-to-advanced AD. The very mild AD group comprised 75 patients (37 men and 38 women) who ranged in age from 51 to 86 years with a mean of 71.2 ± 7.4 years.

Received August 26, 2011; accepted after revision September 23.

From the Department of Nuclear Medicine (H.M., E.I.), Saitama Medical University International Medical Center, Hidaka, Saitama, Japan; Department of Radiology (S.M.), Toho University Omori Medical Center, Ota-ku, Tokyo, Japan; Department of Psychiatry (K.N., T.A.), Graduate School of Comprehensive Human Sciences, University of Tsukuba, Tsukuba, Ibaraki, Japan; Research Association for Biotechnology (F.Y.), Minato-ku, Tokyo, Japan; and Department of Radiology (N.S.), National Center Hospital, National Center of Neurology and Psychiatry, Kodaira, Tokyo, Japan.

This work was supported by a Grant-in-Aid for Scientific Research, Ministry of Education, Culture, Sports, Science and Technology, Japan (21591578).

Please address correspondence to Hiroshi Matsuda, MD, Department of Nuclear Medicine, Saitama Medical University International Medical Center, 1397-1, Yamane Hidaka, Saitama, Japan; e-mail: matsudah@saitama-med.ac.jp


Indicates open access to non-subscribers at www.ajnr.org


Indicates article with supplemental on-line tables.

http://dx.doi.org/10.3174/ajnr.A2935

At the initial visit, they had no apparent loss in general cognitive, behavioral, or functional status and corresponded to the criteria of the amnestic type of MCI[8] or 0.5 in the Clinical Dementia Rating.[9] The MMSE score ranged from 24 to 29 (mean, 25.7 ± 1.5). During the subsequent follow-up period of 2–6 years, the subjects showed progressive cognitive decline and eventually fulfilled the diagnosis of probable AD. The mild and moderate-to-advanced AD groups comprised 30 patients (8 men and 22 women, 71.4 ± 6.8 years of age) and 41 patients (20 men and 21 women, 71.3 ± 7.7 years of age), respectively. The MMSE score ranged from 20 to 25 (mean, 21.4 ± 1.3) and from 6 to 19; (mean, 15.0 ± 3.5) for the mild and moderate-to-advanced AD groups, respectively. Eighty-one of these patients with AD (48 very mild, 11 mild, and 22 moderate-to-advanced) underwent follow-up MRI studies at an interval of 1–4 years for, at most, 6 years (mean, 3.3 ± 1.2 years), and most patients in the very mild and mild AD groups moved to a more advanced group during the follow-up period. Consequently, the total of MRI studies was 89, 57, and 123 for the very mild, mild, and moderate-to-advanced AD groups.

Eighty age-matched control subjects (37 men and 43 women) were healthy volunteers with no memory impairment or cognitive disorders. They ranged in age from 54 to 86 years with a mean of 70.4 ± 7.8 years. Their performance was within normal limits both on the Wechsler Memory Scale–Revised and the Wechsler Adult Intelligence Scale–Revised. Their MMSE scores ranged from 26 to 30 (mean, 29.1 ± 1.2). They did not differ in age or education from the patients with AD. Additionally, 25 healthy volunteers (15 men and 10 women; mean, 31.1 ± 7.8 years of age) participated in this study for creation of a customized template for spatial normalization in the statistical image analysis. The ethics committee approved this study, and all subjects provided informed consent to participate. None of them had asymptomatic cerebral infarction detected by T2-weighted MRI.

All subjects underwent an MRI study on a 1.5T Vision Plus imager (Siemens, Erlangen, Germany). One hundred forty 3D sections of a T1-weighted magnetization-prepared rapid acquisition of gradient echo sequence were obtained in a sagittal orientation as 1.2-mm thick sections (FOV = 23, TR = 9.7 ms, TE = 4 ms, flip angle = 12°, and TI = 300 ms, with no intersection gaps).

First, to define a target VOI for early diagnosis of AD, we performed a group comparison between 30 patients (14 men and 16 women; mean age, 73.8 ± 4.8 years) randomly chosen in the present very mild AD group and the present 40 healthy controls group (19 men and 21 women; mean age, 70.8 ± 8.5 years). Using the latest version of SPM8 (Wellcome Department of Imaging Neuroscience, London, United Kingdom), we segmented MRIs into gray matter, white matter, and CSF images by a unified tissue-segmentation procedure after image-intensity nonuniformity correction. These segmented gray matter images were then spatially normalized to the customized template in the standardized anatomic space by using DARTEL (Wellcome Department of Imaging Neuroscience).[10] The customized template for DARTEL was created from the aforementioned 25 healthy young subjects. To preserve gray matter volume within each voxel, we modulated the images by the Jacobean determinants derived from the spatial normalization by DARTEL and then smoothed them by using an 8-mm FWHM Gaussian kernel. To compare the present analysis by using SPM8 plus DARTEL with the previously reported analysis,[6] we also defined a target VOI by using an old SPM version, SPM2 (Wellcome Department of Imaging Neuroscience) between the same 2 groups. Group comparisons by SPM were assessed by using the family-wise error at a threshold of $P < .05$, corrected for multiple comparisons.

A stand-alone software program running on Windows for VBM analysis by SPM8 plus DARTEL was developed to discriminate patients with AD from healthy controls. First, MRIs were spatially normalized with only a 12-parameter affine transformation to the SPM template so as to correct for differences in brain size. These linearly transformed images were nonlinearly transformed and then modulated to the customized template for DARTEL, followed by smoothing by using an 8-mm FWHM kernel. Each processed gray matter image of the remaining 116 patients with AD and 40 healthy controls was compared with the mean and SD of gray matter images of the 40 healthy volunteers chosen in the group comparison by using voxel-by-voxel z score analysis with and without voxel normalization to global mean intensities (global normalization): z score = ([control mean] − [individual value]) / (control SD). These z score maps were displayed by overlay on tomographic sections and surface rendering of the standardized brain. This program registered the target VOI defined by the aforementioned group comparison. This software program takes 8 minutes 40 seconds for all procedures by using a 64-bit PC with a Core i7 central processing unit and 6-gigabytes memory (Intel, Santa Clara, California).

We determined 4 indicators for characterizing atrophy in a target VOI and in the whole brain: first, the severity of atrophy obtained from the averaged positive z score in the target VOI; second, the extent of a region showing significant atrophy in the target VOI—that is, the percentage rate of the coordinates with a z value exceeding the threshold value of 2 in the target VOI; third, the extent of a region showing significant atrophy in the whole brain—that is, the percentage rate of the coordinates with a z value exceeding the threshold value of 2 in the whole brain; and fourth, the ratio of the extent of a region showing significant atrophy in the target VOI to the extent of a region showing significant atrophy in the whole brain. The utility of these indicators for this discrimination of AD from healthy controls has been reported in previous MRI[6] and SPECT studies.[11]

These 4 indicators were obtained under 2 conditions, with or without global normalization. Using the values of the 4 indicators as the threshold, we determined ROC curves for discrimination of patients with AD from healthy volunteers by using JMP 7.0 (SAS Institute, Cary, North Carolina). The program calculates the area under the ROC curves, sensitivity, specificity, and accuracy. Moreover, the age effects of AD onset on these 4 indicators and the results of the ROC were investigated in the very mild AD group classified into 2 subgroups with an age threshold of 65: the early-onset subgroup (16 patients, 9 men and 7 women; mean age, 58.0 ± 4.6 years) and the late-onset subgroup (29 patients, 14 men and 15 women; mean age, 73.8 ± 4.4 years).

Results

The group comparison by SPM8 plus DARTEL demonstrated significant decline of gray matter volume in the left (Talairach coordinates −24,−10,−14, x,y,z; z = 7.37 and 6.95 without and with global normalization, respectively) and the right (24,10,14, x,y,z; z = 7.42 and 7.05 without and with global normalization, respectively) parahippocampal gyri in patients with very mild AD (Fig 1). These bilateral regions involve the entorhinal cortex, head to tail of the hippocampus, and amygdala and are delineated as a target VOI for AD. Group comparison by SPM2 showed significant decline of gray matter volume in the left (−18, −7, −16, x,y,z; z = 6.18) and right

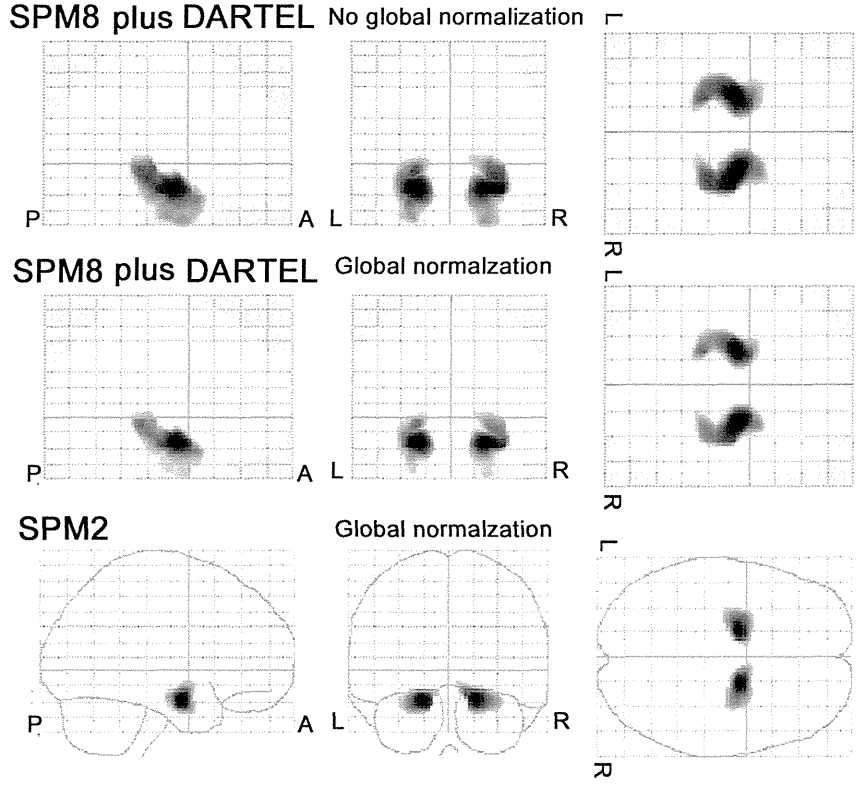

Fig 1. Group comparison of gray matter volume by SPM8 plus DARTEL and SPM2 between 30 patients with very mild AD and 40 healthy age-matched volunteers. The SPM8 plus DARTEL analysis demonstrates significant decline of gray matter volume in the bilateral medial temporal structures both with and without global normalization in patients with very mild AD. The cluster shape is very close to the anatomic configuration of the medial temporal structures involving the entorhinal cortex, amygdala, and hippocampal formation from head to tail. Although the SPM 2 analysis demonstrates a significant decline of gray matter volume in the bilateral medial temporal structures, the cluster is confined to the anterior parts of the medial temporal structures.

Table 1: Values of 4 indicators for characterizing atrophy[a]

		SPM8 plus DARTEL				SPM2			
		Target VOI			Whole-Brain	Target VOI			Whole-Brain
Group	Global Normalization	Severity	Extent (%)	Ratio	Extent (%)	Severity	Extent (%)	Ratio	Extent (%)
Healthy controls	−	0.7 ± 0.5	4.4 ± 9.8	0.8 ± 1.5	2.5 ± 4.7	NA	NA	NA	NA
	+	0.7 ± 0.3	2.0 ± 4.9	1.3 ± 2.8	1.4 ± 0.9	0.5 ± 0.3	1.8 ± 7.3	0.5 ± 1.8	2.6± 3.1
Very mild AD	−	1.8 ± 0.9[b]	39.0 ± 35.5[b]	9.9 ± 8.9[b]	5.4 ± 7.6[b]	NA	NA	NA	NA
	+	2.2 ± 0.9[b]	49.2 ± 30.2[b]	12.9 ± 7.8[b]	4.1 ± 2.5[b]	1.6 ± 1.0[b]	30.8 ± 32.1[b]	6.7 ± 7.8[b]	5.4 ± 3.7[b]
Mild AD	−	2.2 ± 0.7[b]	53.7 ± 29.8[b]	12.8 ± 8.8[b]	5.5 ± 5.1[b]	NA	NA	NA	NA
	+	2.7 ± 0.8[b]	63.7 ± 25.8[b]	15.4 ± 7.8[b]	4.3 ± 1.9[b]	2.1 ± 1.1[b]	42.0 ± 32.3[b]	9.6 ± 9.2[b]	5.4 ± 3.0[b]
Moderate-to-advanced AD	−	2.8 ± 1.0[b,c,d]	72.2 ± 26.5[b,c,d]	8.4 ± 7.2[b]	15.1 ± 14.0[b,c,d]	NA	NA	NA	NA
	+	3.0 ± 1.0[b,c]	68.7 ± 24.1[b,c]	11.7 ± 6.7[b,d]	7.1 ± 3.7[b,c,d]	2.6 ± 1.4[b,c]	56.3 ± 33.2[b,c]	7.6 ± 6.2[b]	9.0 ± 5.0[b,c,d]

Note:—NA indicates not applicable; +, presence; −, absence.
[a] Tukey honest significance test in each condition of global normalization.
[b] $P < .001$ versus healthy controls.
[c] $P < .001$ versus very mild AD group.
[d] $P < .001$ versus mild AD group.

(18, −5,15, x,y,z; $z = 5.86$) parahippocampal gyri (Fig 1). The cluster size was smaller in SPM2 than in SPM8 plus DARTEL.

The patients with AD showed significantly ($P < .001$, Tukey honest significance test) greater values than healthy controls in all 4 indicators in both SPM8 plus DARTEL and SPM2 analysis (Table 1). The mild AD group showed not significant but greater values of all 4 indicators than the very mild AD group. The moderate-to-advanced AD group showed significantly ($P < .001$) greater values of severity and extent for the target VOI and extent for the whole brain than the very mild AD group. In contrast, the ratio for the target VOI in the moderate-to-advanced AD group was lower than that in the mild AD group and almost equal to that in the very mild AD group. Global normalization in SPM8 plus DARTEL analysis elevated the severity and ratio for the target VOI and diminished the extent for the whole brain in all AD groups. The SPM2 analysis showed lower values in severity, extent, and ratio for a target VOI and greater values in extent for the whole brain than the SPM8 plus DARTEL analysis.

In the SPM8 plus DARTEL analysis, better ROC results were obtained in the condition with than without global normalization, particularly in specificity (On-line Table 1). Of the

Table 2: Values of 4 indicators in early- and late-onset subgroups in very mild AD

		SPM8 plus DARTEL				SPM2			
		Target VOI			Whole-Brain	Target VOI			Whole-Brain
Global Normalization	Onset	Severity	Extent (%)	Ratio	Extent (%)	Severity	Extent (%)	Ratio	Extent (%)
−	Early	1.5 ± 0.7	25.3 ± 31.1	3.8 ± 3.8	5.1 ± 4.9	NA	NA	NA	NA
−	Late	1.9 ± 0.9	43.8 ± 35.6	5.9 ± 8.4	11.6 ± 9.5	NA	NA	NA	NA
+	Early	1.9 ± 0.7	37.4 ± 26.2	9.5 ± 6.0	4.1 ± 1.7	1.4 ± 1.0	24.4 ± 34.6	4.7 ± 5.5	3.8 ± 2.4
+	Late	2.3 ± 0.9	53.6 ± 30.7	14.1 ± 8.1	4.1 ± 2.7	1.7 ± 1.0	33.2 ± 31.2	7.5 ± 8.5	6.0 ± 3.9

Note:—NA indicates not applicable; +, presence; −, absence.

4 indicators, the severity and extent for the target VOI with global normalization showed almost equal and high accuracy. Even in the very mild AD group, the severity showed a high accuracy of 91.6%, increasing to 95.8% in the mild AD group and 98.2% in the moderate-to-advanced AD group. SPM8 plus DARTEL showed better ROC results for all 4 indicators than SPM2.

Although the early-onset subgroup showed lower values of indicators for the target VOI than the late-onset subgroup (Table 2), global normalization elevated these indicators evenly in the early- and late-onset subgroups. These indicators were largely stable before and after global normalization in healthy controls. Consequently, ROC results in SPM8 plus DARTEL revealed equal accuracy after global normalization between these 2 subgroups (Online Table 2). In contrast, SPM2 analysis showed approximately 10% lower accuracy in the early-onset subgroup than that in the late-onset subgroup when using the severity score.

In each of 81 follow-up patients with AD, the severity score in a target VOI gradually increased from the baseline to follow-up studies. The annual increase of the severity score after global normalization was 0.27 ± 0.15.

Representative cross-sectional and longitudinal studies for SPM8 plus DARTEL analysis are demonstrated in Figs 2 and 3, respectively.

Discussion

Using severity as an indicator, we obtained a high sensitivity of 86.4% and extremely high specificity of 97.5%, resulting in an accuracy of 91.6% for discrimination of patients with very mild AD from healthy controls in the SPM8 plus DARTEL analysis. Extremely high specificity mainly contributed to this high accuracy. In the SPM2 analysis, ROC analysis presented 5% lower sensitivity and approximately 13% lower specificity compared with those in the SPM8 plus DARTEL analysis. Kawachi et al[12] reported 82.9% in both sensitivity and specificity in the patients with very mild AD in a similar VBM study by using an older SPM version, SPM99. This better specificity may result from application of the SPM8 plus DARTEL algorithm. This DARTEL algorithm can provide more precise spatial normalization to the template than the conventional algorithm.[10,13]

This improvement in the preciseness of the spatial normalization was confirmed by group comparison for determining a target VOI. The SPM8 plus DARTEL results showed significantly decreased volume with anatomically precise configura-

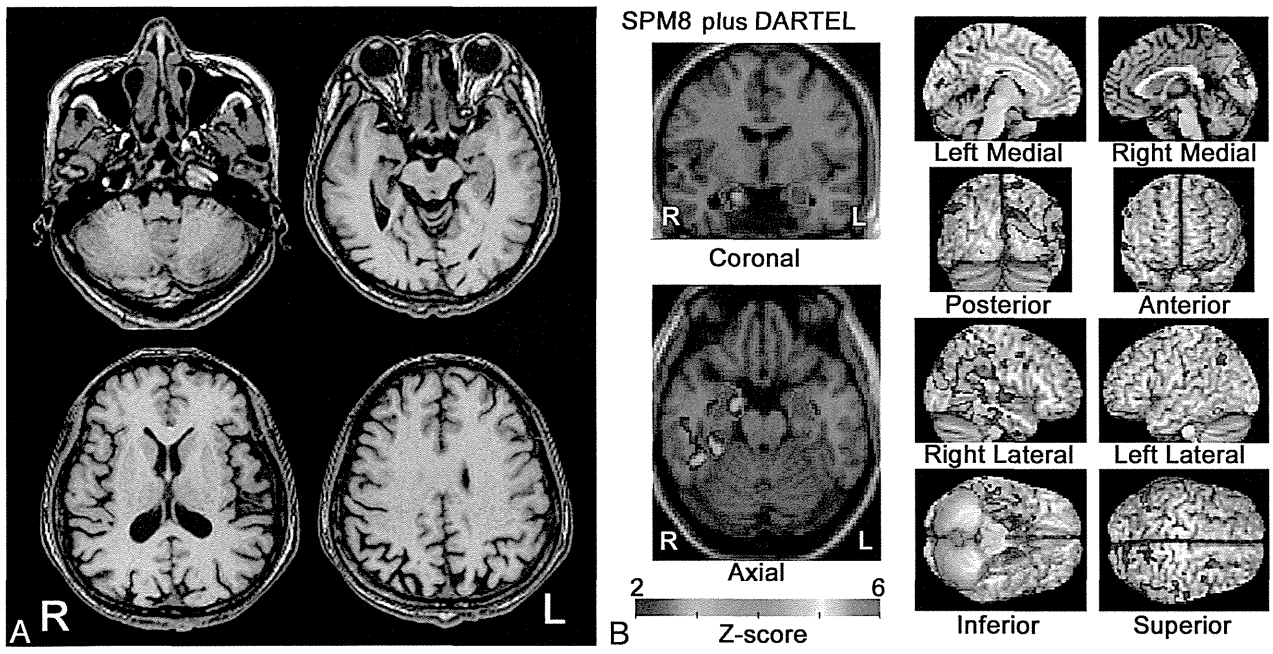

Fig 2. Cross-sectional VBM study by using SPM8 plus DARTEL. *A*, MR image of a 52-year-old woman with an MMSE score of 27. One year later the MMSE score declined to 19. *B*, SPM8 plus DARTEL analysis with global normalization reveals a significant decrease of gray matter volume in the right entorhinal area. Colored areas with *z* scores of >2 are overlaid as significantly atrophied regions on tomographic sections and cortical surface of the standardized MRI template. A target VOI in the medial temporal structures is demarcated with purple lines. The right temporoparietal cortex also shows extensive significant atrophy.

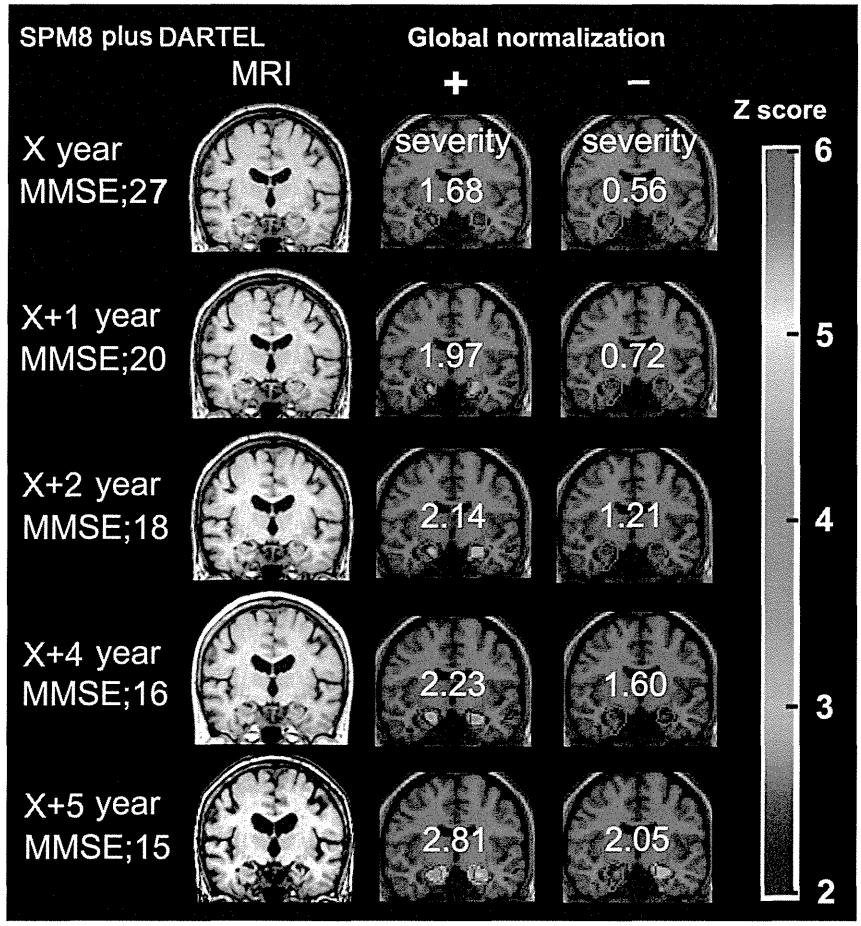

Fig 3. Longitudinal VBM studies by using SPM8 plus DARTEL. A 63-year-old woman with an MMSE score of 27 at the first visit was followed up for 6 years. One year later, the MMSE score decreased to 20 and gradually decreased thereafter. VBM analysis with global normalization reveals significant atrophy in the bilateral medial temporal areas even at the time of the initial study. Then the *z* score in a target VOI increased step by step with time. In contrast, analysis without global normalization does not demonstrate significant atrophy in the medial temporal areas for the first 3 years. Severity scores as an indicator for characterizing atrophy in the medial temporal structures are shown.

tion of the medial temporal structures involving the entorhinal cortex, amygdala, and total hippocampal formation. Takahashi et al[14] demonstrated almost identical results by using SPM8 plus DARTEL. The present SPM results by using conventional VBM by SPM2 showed decreased gray matter volume mainly in the anterior parts of the parahippocampal gyri with a less precise configuration. The severity score proved to be useful for longitudinal studies as well. The annual increase of this score may be indicative of disease progression.

The modulation in VBM allows comparison of the absolute amount of gray matter.[15] The step of global normalization allows correction of the absolute amount of gray matter for individual total brain volume. Comparison of discrimination performance demonstrated better results in the condition with than without global normalization. This difference in discrimination performance may arise from the well-known fact of selective atrophy in the medial temporal structures in AD.[1,4-6,16,17] Even if the absolute amount of gray matter of the medial temporal structures is decreased, a concomitant decrease in the total volume of gray matter would decrease specificity. The specificity in ROC analysis of the severity for the target VOI was 17% lower in the condition without than with global normalization in very mild AD. The degree of selective atrophy in the medial temporal areas can be assessed by the ratio as an indicator. In patients with AD, more than 10-fold selective atrophy was observed in the medial temporal areas compared with the whole brain in SPM8 plus DARTEL. Global normalization enhanced this ratio. Progression of neocortical atrophy would result in the decline of this ratio in advanced AD. This indicator may be useful for differentiation of AD from other neuropsychiatric diseases manifesting dementia.

The early-onset subgroup showed milder atrophy in the medial temporal structures than the late-onset subgroup. This is in line with several previous reports in which late-onset subgroups showed greater atrophy in the medial temporal structures than the early-onset subgroups.[16,17] However global normalization in SPM8 plus DARTEL extended the difference of indicators for a target VOI evenly in the early-onset and late-onset subgroups from indicators in healthy controls. This extension led to almost equal accuracy for discrimination of early-onset and late-onset very mild AD from healthy controls. This global normalization procedure may make it possible to use a common target VOI irrespective of age at onset of AD.

Thus the present study made it clear that the global normalization procedure in VBM by using SPM8 plus DARTEL has advantages in enhancing the discrimination power of diagnosing AD. However lower values of the extent for the whole brain after global normalization would underestimate neocor-

tical atrophy. The extent for the whole brain without global normalization may be useful for accurately evaluating the degree of neocortical atrophy.

This study is not without limitations. First, we should investigate whether this 1-site study is applicable to multicenter studies. Second, evaluation of the reproducibility of the present VBM technique may be necessary for longitudinal studies. Third, we investigated patients with amnestic MCI who all converted to AD. The outcome for any patient with MCI is uncertain because many subjects remain stable or even revert to a normal state, while others progress to dementia. Accordingly, the predictive study by using this VBM approach is much more important for MCI conversion to AD. Fourth, the single target VOI was used irrespective of age at onset of AD. A similar VBM study by Ishii et al[18] recommended the use of a target VOI involving not only medial temporal structures but also parietal and posterior cingulate cortices and precunei in early-onset AD. Although this software program presented the same accuracy between early- and late-onset very mild AD subgroups, we may have to investigate a more appropriate target VOI from a larger number of patients with early-onset AD. However, incorporation of 2 types of target VOIs for early- and late-onset AD into a software program may confound the program user in the selection of a target VOI in the case of follow-up studies on an approximately 65-year-old patient.

Conclusions

We proposed an automatic VBM software program of structural MRI for discrimination between patients with probable AD from the very-mild- to advanced stages and age-matched healthy controls. Application of the SPM8 plus DARTEL analysis to this software program provided a high accuracy of 91.6% for discrimination of patients with very mild AD from healthy controls by using a target VOI located in medial temporal structures. Equal accuracies were obtained in early-onset and late-onset very mild AD subgroups. This software program may be useful for early diagnosis and longitudinal evaluation of AD.

References

1. Frisoni GB, Fox NC, Jack CR Jr, et al. **The clinical use of structural MRI in Alzheimer disease.** *Nat Rev Neurol* 2010;6:67–77
2. Gómez-Isla T, Price JL, McKeel DW Jr, et al. **Profound loss of layer II entorhinal cortex neurons occurs in very mild Alzheimer's disease.** *J Neurosci* 1996;16:4491–500
3. Ashburner J, Friston KJ. **Voxel-based morphometry: the methods.** *Neuroimage* 2000;11:805–21
4. Baron JC, Chételat G, Desgranges B, et al. **In vivo mapping of gray matter loss with voxel-based morphometry in mild Alzheimer's disease.** *Neuroimage* 2001;14:298–309
5. Whitwell JL, Josephs KA, Murray ME, et al. **MRI correlates of neurofibrillary tangle pathology at autopsy: a voxel-based morphometry study.** *Neurology* 2008;71:743–49
6. Hirata Y, Matsuda H, Nemoto K, et al. **Voxel-based morphometry to discriminate early Alzheimer's disease from controls.** *Neurosci Lett* 2005;382:269–74
7. McKhann G, Drachman D, Folstein M, et al. **Clinical diagnosis of Alzheimer's disease: report of the NINCDS-ADRDA work group under the auspices of Department of Health and Human Services taskforce on Alzheimer's disease.** *Neurology* 1984;34:939–44
8. Petersen RC, Doody R, Kurz A, et al. **Current concepts in mild cognitive impairment.** *Arch Neurol* 2001;58:1985–92
9. Hughes CP, Berg L, Danziger WL, et al. **A new clinical scale for the staging of dementia.** *Br J Psychiatry* 1982;140:566–72
10. Ashburner J. **A fast diffeomorphic image registration algorithm.** *Neuroimage* 2007;38:95–113
11. Matsuda H, Mizumura S, Nagao T, et al. **Automated discrimination between very early Alzheimer disease and controls using an easy Z-score imaging system for multicenter brain perfusion single-photon emission tomography.** *AJNR Am J Neuroradiol* 2007;28:731–36
12. Kawachi T, Ishii K, Sakamoto S, et al. **Comparison of the diagnostic performance of FDG-PET and VBM-MRI in very mild Alzheimer's disease.** *Eur J Nucl Med Mol Imaging* 2006;33:801–09
13. Pereira JM, Xiong L, Acosta-Cabronero J, et al. **Registration accuracy for VBM studies varies according to region and degenerative disease grouping.** *Neuroimage* 2010;49:2205–15
14. Takahashi R, Ishii K, Miyamoto N, et al. **Measurement of gray and white matter atrophy in dementia with Lewy bodies using diffeomorphic anatomic registration through exponentiated lie algebra: a comparison with conventional voxel-based morphometry.** *AJNR Am J Neuroradiol* 2010;31:1873–78
15. Karas GB, Burton EJ, Rombouts SA, et al. **A comprehensive study of gray matter loss in patients with Alzheimer's disease using optimized voxel-based morphometry.** *Neuroimage* 2003;18:895–907
16. Matsunari I, Samuraki M, Chen WP, et al. **Comparison of 18F-FDG PET and optimized voxel-based morphometry for detection of Alzheimer's disease: aging effect on diagnostic performance.** *J Nucl Med* 2007;48:1961–70
17. Frisoni GB, Pievani M, Testa C, et al. **The topography of grey matter involvement in early and late onset Alzheimer's disease.** *Brain* 2007;130:720–30
18. Ishii K, Kawachi T, Sasaki H, et al. **Voxel-based morphometric comparison between early- and late-onset mild Alzheimer's disease and assessment of diagnostic performance of z score images.** *AJNR Am J Neuroradiol* 2005;26:333–40

Citation: Transl Psychiatry (2012) 2, e178; doi:10.1038/tp.2012.108

www.nature.com/tp

Absence of age-related prefrontal NAA change in adults with autism spectrum disorders

Y Aoki[1], O Abe[2], N Yahata[1,3], H Kuwabara[4], T Natsubori[1], N Iwashiro[1], Y Takano[1], H Inoue[1], Y Kawakubo[4], W Gonoi[5], H Sasaki[5], M Murakami[5], M Katsura[5], Y Nippashi[5], H Takao[5], A Kunimatsu[5], H Matsuzaki[6], KJ Tsuchiya[6], N Kato[7], K Kasai[1] and H Yamasue[1,8]

Atypical trajectory of brain growth in autism spectrum disorders (ASDs) has been recognized as a potential etiology of an atypical course of behavioral development. Numerous neuroimaging studies have focused on childhood to investigate atypical age-related change of brain structure and function, because it is a period of neuron and synapse maturation. Recent studies, however, have shown that the atypical age-related structural change of autistic brain expands beyond childhood and constitutes neural underpinnings for lifelong difficulty to behavioral adaptation. Thus, we examined effects of aging on neurochemical aspects of brain maturation using 3-T proton magnetic resonance spectroscopy (^{1}H-MRS) with single voxel in the medial prefrontal cortex (PFC) in 24 adult men with non-medicated high-functioning ASDs and 25 age-, IQ- and parental-socioeconomic-background-matched men with typical development (TD). Multivariate analyses of covariance demonstrated significantly high *N*-acetylaspartate (NAA) level in the ASD subjects compared with the TD subjects ($F = 4.83$, $P = 0.033$). The low NAA level showed a significant positive correlation with advanced age in the TD group ($r = -0.618$, $P = 0.001$), but was not evident among the ASD individuals ($r = 0.258$, $P = 0.223$). Fisher's *r*-to-*z* transformation showed a significant difference in the correlations between the ASD and TD groups ($Z = -3.23$, $P = 0.001$), which indicated that the age–NAA relationship was significantly specific to people with TD. The current ^{1}H-MRS study provided new evidence that atypical age-related change of neurochemical aspects of brain maturation in ASD individuals expands beyond childhood and persists during adulthood.
Translational Psychiatry (2012) **2,** e178; doi:10.1038/tp.2012.108; published online 23 October 2012

Introduction

Atypical growth trajectory has been recognized in individuals with autism spectrum disorders (ASDs), both at the behavioral and neural levels. Previous meta-analyses have repeatedly reported that overall brain size is slightly reduced at birth, dramatically increases within the first year of life, but then gradually plateaus into adulthood.[1,2] It has been suggested that there is a dynamic curve of atypical trajectory during the first year of life, and the latest longitudinal studies have shown different developmental curves in brain structure between infants with ASDs and typical development (TD) during this period.[3,4] The aberrant brain growth has been shown to occur in many brain areas, but particularly in the frontal lobe.[1,5,6] Several studies employing neuroimaging have shown that among many other functions,[7,8] the PFC is critically important in mentalizing,[9] empathy,[10] irony comprehension,[11] social judgment[12] and self-referencing,[13,14] which are impaired and constitute a core feature of ASDs.

Although the period of dynamic change in infantile autistic brain has been investigated so far, cumulative data from structural and functional neuroimaging studies have demonstrated that those atypical age-related changes expand beyond childhood. Emerging studies that recruited adolescents with ASDs showed different aging effects on brain structure between subjects with ASDs and TD.[15] Furthermore, several studies have demonstrated atypical age-related changes in brain structure and function, especially in the frontal lobe[16–18] and tract involving the frontal lobe,[19] even during adulthood in people with ASDs. Although these atypical age-related changes at the neural level may constitute substrates for lifelong behavioral difficulty in people with ASDs,[20] such changes during adulthood have rarely been reported on brain neurochemical aspects.

^{1}H-magnetic resonance spectroscopy (^{1}H-MRS) is a non-invasive neuroimaging technique that estimates specific chemical metabolite measures *in vivo*.[21] Although what the measured metabolite levels reflect is an area of debate, previous studies have used ^{1}H-MRS to quantify glutamine/glutamate (referred to collectively as 'Glx'); *N*-acetylaspartate (NAA), a marker of neuronal density, plasticity and function; choline-containing compounds (Cho), a measure primarily reflecting the constituents of cell membranes; creatine and phosphocreatine (Cre), a measure of cellular energy metabolism; and myo-inositol (mI), a major osmolite precursor

[1]Department of Neuropsychiatry, Graduate School of Medicine, The University of Tokyo, Tokyo, Japan; [2]Department of Radiology, Nihon University School of Medicine, Tokyo, Japan; [3]The GCOE, The University of Tokyo, Tokyo, Japan; [4]Department of Child Psychiatry Graduate School of Medicine, The University of Tokyo, Tokyo, Japan; [5]Department of Radiology, Graduate School of Medicine, The University of Tokyo, Tokyo, Japan; [6]Research Center for Child Mental Development, Hamamatsu University School of Medicine, Hamamatsu, Japan; [7]Department of Neuropsychiatry, Showa University School of Medicine, Tokyo, Japan and [8]Japan Science and Technology Agency, CREST, Tokyo, Japan
Correspondence: Professor H Yamasue, Department of Neuropsychiatry, Graduate School of Medicine, The University of Tokyo, 7-3-1 Hongo, Bunkyo-ku, Tokyo 113-8655, Japan.
E-mail: yamasue-tky@umin.ac.jp
Keywords: anterior cingulate; Asperger syndrome; autistic disorder; case–control; human; pervasive developmental disorder
Received 16 July 2012; revised 23 August 2012; accepted 31 August 2012

for phosphoinositides involved in the second messenger system.[22,23]

Consistent with atypical age-related brain morphological change in people with ASDs, our recent meta-analysis of ^{1}H-MRS studies involving ASD individuals also robustly demonstrated age-related diminishment of NAA reduction in the frontal lobe.[24] The meta-analysis showed a significant frontal NAA reduction in groups with ASDs compared with TD during childhood, and further demonstrated a significant linear correlation between older age and a smaller magnitude of the frontal NAA decrease. Thus, the meta-analysis showed no significant difference in NAA level between ASD and TD subjects during adulthood. However, because of a lack of sufficient number of studies recruiting adults with ASDs in the meta-analysis, it remains unclear whether this atypical relationship between NAA and age continues during adulthood. In contrast, in people with TD, age-dependent NAA reduction in the frontal lobe during adulthood has been revealed by a number of cross-sectional ^{1}H-MRS studies[25–29] and a meta-analysis of ^{1}H-MRS studies.[30]

Taken together, it was expected that adults with ASD would show atypical age–NAA relationship (that is, lack of age-related decrease in frontal NAA) in the PFC. As a result, an absence of decrease, or even increase, in prefrontal NAA level would be predicted in adults with ASD compared with the matched TD controls, while previous studies have demonstrated a significant decrease in the prefrontal NAA of children with ASD.[24] To test these hypotheses with minimizing potential confounders, the present study utilized 3-T ^{1}H-MRS to examine differences in the medial prefrontal NAA levels between non-medicated high-functioning adult males with ASD and age-, IQ- and parental-socioeconomic (SES)-background-matched TD male subjects. Then, we examined correlations between the medial prefrontal NAA levels and age in the diagnostic groups separately. The statistical significance of diagnostic difference in the correlation coefficients was further examined.

Materials and methods

Participants. The inclusion and exclusion criteria, diagnostic protocols and clinical assessments of study participants were the same as our previous study.[12] In all, 24 adult males (mean age = 29.5, range = 20–44 years) with a clinical diagnosis of high-functioning ASDs were recruited from the outpatient services of The University of Tokyo Hospital. The ASD participants met the following criteria to be included: no psychotropic medication and IQ >80. The ASD participants were diagnosed according to the strict criteria included in the Diagnostic and Statistical Manual-Revision IV, requiring consensus based on more than 2 months of longitudinal follow-up examinations by at least two trained child–adolescent psychiatrists with more than 10 years of clinical experience (HY and NK). The diagnoses were further confirmed using the validated Japanese version of Autism Diagnostic Interview-Revised (ADI-R) by another trained child adolescent psychiatrist (HK).[31,32] Of the participants not reaching the threshold in the ADI-R social domain, the Childhood Autism Rating Scale[33] was employed to confirm the diagnosis of ASDs. Previous studies have suggested that individuals classified as autistic according to both ADI-R and Childhood Autism Rating Scale had significantly lower IQ than those classified with the Childhood Autism Rating Scale only.[34] It is reasonable that the current high-functioning ASD participants who did not meet the ASD criteria based on ADI-R, which was rated based on descriptive information by caregivers, could be classified as ASDs based on the Childhood Autism Rating Scale, which was rated by clinicians based on direct observations on behavior.[35] All of the ASD participants were interviewed by a trained psychiatrist (HY) to screen for the presence or absence of comorbid neuropsychiatric disorders using the Structured Clinical Interview for Diagnostic and Statistical Manual-Revision IV axis I disorder. In all, 25 age-, IQ- and parental-SES-matched, TD adult males were employed as controls. The ethics committee of The University of Tokyo Hospital approved this study (No. 397). After a complete explanation of the study to the subjects, written informed consent was obtained from every participant.

The exclusion criteria for both groups were: current or past neurological comorbidity, traumatic brain injury with any known cognitive consequences or loss of consciousness for more than 5 min, a history of electroconvulsive therapy and substance abuse or addiction. An additional exclusion criterion for the control group was a history of psychiatric disease in the subjects themselves or a family history of axis I disorder in their first-degree relatives.

To detect the diagnostic difference in age–NAA relationship, power was based on previous MRS studies comparing correlation between NAA level in volume of interest (VOI) at the similar location and its functional or behavioral substrates of adults with ASDs with those with TD.[36,37] Since the effect size q for difference between Pearson's correlation coefficient of these previous studies ranged from 0.75 to 1.26, the required total sample sizes for 80% power at a 0.05 level of significance ranged from 26 to 62. Thus, in the current study, we collected data from more than 44 individuals, which is the median of the calculated range.

Questionnaire measures. Handedness was determined using the Edinburgh Handedness Inventory,[38] with a laterality index of >0.5 used as the cutoff for right-handedness. Participants whose laterality index score ranged from -0.5 to 0.5 were defined as mixed-handedness. All of the ASD and TD participants completed valid Japanese translations[39] of the 50-item Autism-Spectrum Quotient.[40] The maximum total score of Autism-Spectrum Quotient was 24 in the controls, while the cutoff threshold was defined as 34 points.[40] The IQ of the TD controls was estimated using the Japanese version of the National Adult Reading Test.[41] Although the National Adult Reading Test can represent the full IQ in TD participants, it is problematic for ASD participants because of their well-known imbalanced intellectual abilities. Therefore, IQ was evaluated using the full scale of the Wechsler Adult Intelligence Scale Revised Japanese version[42] for participants with ASDs. The SES of participants and their parents were assessed using the Hollingshead Scale.[43]

MRI acquisition. Magnetic resonance imaging (MRI) data were obtained using a 3-T scanner (GE Signa HDxt, Waukesha, WI, USA). All the participants from both the diagnostic groups were scanned during the same period, between January 2010 and November 2011. There was no upgrade of MRI scanner or software version in this period. An 8-channel brain-phased array coil was used for both MRI and ^{1}H-MRS. A sagittal localizer scan was obtained first, followed by the axial T2-weighted images (echo time (TE) = 82.32 ms, repetition time (TR) = 4400 ms, field of view = 240 × 240 mm^2, matrix = 256 × 256, slice thickness = 2.5 mm, number of axial slices = 62) for positioning the voxel of interest (VOI). Three-dimensional fast-spoiled gradient recalled acquisition with steady state (TE = 1.94 ms, TR = 6.80 ms, field of view = 240 × 240 mm^2, matrix = 256 × 256, flip angle = 20°, slice thickness = 1.0 mm, number of axial slices = 176) was acquired for tissue segmentation correction. Trained neuroradiologists (OA, WG, HS, MM, MK, HT or YN) evaluated the MRI scans and found no gross abnormalities in any of the subjects.

^{1}H-MRS acquisition. The stimulated echo acquisition mode (TR = 3000 ms, TE = 15 ms, mixing time = 13.7 ms, 128 water-suppressed and 8 water-unsuppressed averages) was applied to obtain proton MR spectrum. The definition of positioning of the VOI was based on our previous study.[44] Briefly, in the mid-sagittal slice based on the T2-weighted image, the VOI (20 × 20 × 20 mm^3) was placed closest to the most anterior part of the genu of the corpus callosum with the center of the VOI, containing predominantly the gray matter of the medial PFC (mainly anterior cingulate and paracingulate gyri) bilaterally (Figure 1a).

Spectrum quantification. All spectra were quantified with an LCModel (ver. 6.1-4F). The raw spectral data were read into an LCMgui by which spectrum processing were performed automatically. Based on the comparison of *in vitro* spectra with its measurements analyzed with the LCModel basis set, the absolute levels for 17 metabolites, such as NAA, *N*-acetylaspartylglutamate, alanine, γ-amino-butyric acid, aspartate, choline, creatine (total), glutamate, glutamine, glutathione, glycerophosphocholine, glycine, myo-inositol, scyllo-inositol, lactate, phosphocholine and taurine, were estimated from *in vivo* spectra. Among the 17 metabolites, the current study focused on NAA, Cre, Glx (glutamine plus glutamine), mI and Cho (glycerophosphocholine plus phosphocholine). Representative spectra of ASD and TD are shown in Figures 1b and c.

Spectrum quality. All of the metabolite spectra that showed %s.d. > 20% were excluded from the analysis. In addition,

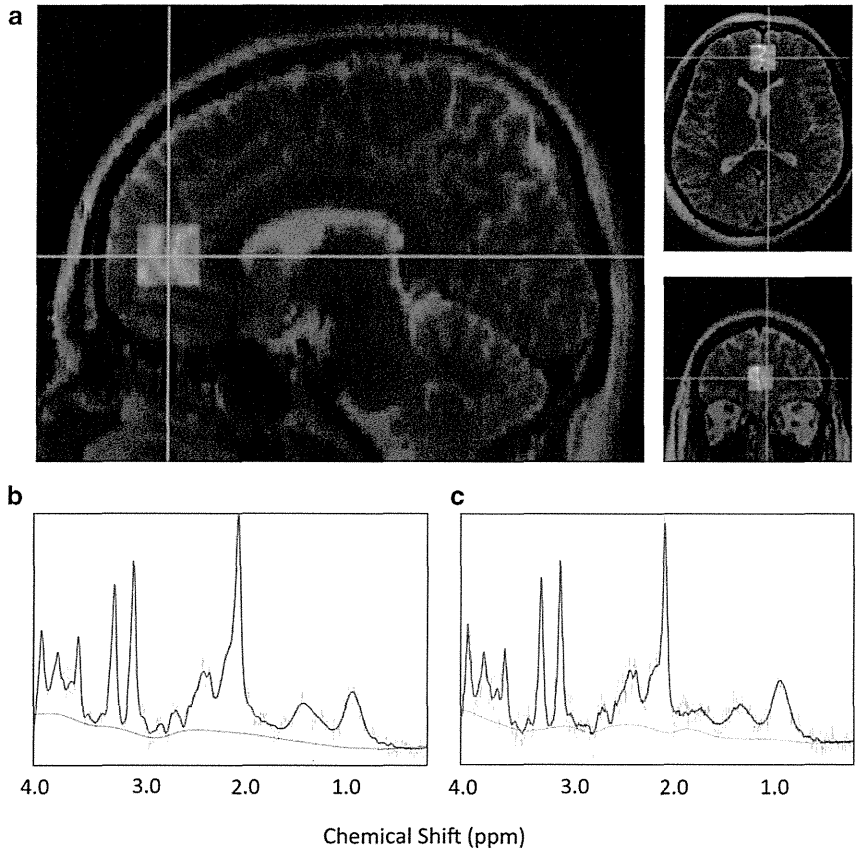

Figure 1 Location of volume of interest (VOI) and representative spectra of 3-T proton magnetic resonance spectroscopy (^{1}H-MRS). (**a**) A T2-weighted brain image in orthogonal slices in a control subject. The square indicates the VOI (20 × 20 × 20 mm^3) voxel in the medial prefrontal cortex, including mainly the pregenual anterior cingulate and paracingulate gyri. (**b** and **c**) Representative medial prefrontal ^{1}H-MRS spectra of autism spectrum disorder (ASD) subject (**b**) or typical development (TD) subject (**c**) as fit by the LCModel.

full-width at half-maximum <0.16 p.p.m. and signal-to-noise ratio (S/N) >3 were used as determinants of spectrum quality required for inclusion. For all the participants, all five metabolites satisfied the criteria for spectrum quality.

Tissue segmentation. Three-dimensional fast-spoiled gradient recalled acquisition with steady state images were used to calculate the volumes of different tissue types (gray matter (GM), white matter (WM) and cerebrospinal fluid (CSF)) by the new segmentation tool of SPM8 (www.fil.ion.ucl.ac.uk/spm). By the tag information of the header of each spectrum file, the center point of VOI was identified. Then, the VOI was reconstructed in the fast-spoiled gradient recalled acquisition with steady state images by tracing the center point. Using SPM8, we co-registered T2-weighted and three-dimensional fast-spoiled gradient recalled acquisition with steady state images, and calculated the volume of GM, WM and CSF. Subsequently, to obtain tissue-contamination-corrected metabolite intensities, each metabolite value was corrected for the CSF content of the VOI using the formula: corrected level = uncorrected level/$(1 - C)$, where C was the fractional CSF content of the VOI.[45]

Statistical method. All statistical analyses were conducted using SPSS 18.0 (SPSS, Chicago, IL, USA). Demographic variables, including age, height, body weight, self-SES, parental-SES, handedness, total Autism-Spectrum Quotient score and IQ, volumes of each tissue component within the VOI (GM, WM and CSF volumes) and indices representing MRS quality (that is, full-width at half-maximum, %s.d. and S/N ratio), were compared using independent two-tailed *t*-tests between ASD and TD subjects. To assess strictly the effect of potential confounders or MRS quality control, significance level was set at $P<0.05$ without correction for multiple comparisons.

For the group comparison of metabolite levels, we employed multivariate analyses of covariance, treated corrected level of each metabolite as a dependent variable (NAA, Cre, Glx, mI and Cho) and diagnosis as a main factor. As the CSF components had already been accounted for by calculating the corrected level, GM and WM components were additionally treated as covariates in the multivariate analyses of covariances to account for the significant difference in the GM within VOI and WM tissue water content between ASD and TD subjects.[46,47] The level of statistical significance was defined as $P<0.05$. As we have *a priori* hypothesis that NAA level in ASDs is deviated from that in TD in adulthood, we did not apply correction for multiple comparisons.

Associations between NAA level and age were analyzed with Pearson's correlation analysis in ASD and TD groups, respectively, and differences in correlations between groups were examined with the Fisher *r*-to-*z* transformation. The significance was reported when *P*-value was <0.05.

The associations between clinical scores, such as ADI-R scores and NAA levels, which showed significant effect of diagnosis, were explored for significance using Pearson's correlation coefficient in the ASD subjects. The significance level was set at $P<0.05$. In addition, Pearson's correlation coefficient between the demographical information (height, body weight, self-SES, parental-SES and IQ) and the NAA levels was also calculated in each group separately. We considered $P<0.05$ as denoting statistical significance to detect effects of potential confounders.

Results

Group difference in demographic characteristics. There were no significant differences between the ASD and control groups in age, body weight, parental-SES and IQ, although the ASD group had significantly lower self-SES and shorter height than controls. The ASD subjects had significantly higher GM ($P=0.006$) and lower CSF ($P=0.003$) contaminations within the VOI (Table 1).

Diagnostic differences in spectral quality and metabolite level. The quality of the spectra obtained from ^{1}H-MRS was good, with a mean (s.d.) S/N ratio reported by the LCModel at 9.96 (2.85) and 11.12 (2.67) in the ASD and TD groups, respectively. Full-width at half-maximums recorded by the LCModel in subjects with ASDs and TD were 0.075 (0.003) and 0.064 (0.019), respectively. %s.d.'s reported by the LCModel in individuals with ASDs and TD were 4.04 (0.93) and 4.67 (1.20) in Cre, 5.84 (1.65) and 6.46 (1.61) in mI, 5.08 (2.23) and 5.08 (1.79) in NAA, 4.08 (1.22) and 4.04 (0.75) in Cho and 7.40 (2.04) and 7.46 (1.56) in Glx, respectively. Independent *t*-tests demonstrated that there were no significant differences in spectral quality between the ASD and TD groups in S/N ratio ($P=0.147$) and full-width-at-half-maximum ($P=0.107$). With regard to %s.d.'s, independent *t*-test demonstrated no significant difference in mI ($P=0.192$), NAA ($P=0.995$), Cho ($P=0.896$) and Glx ($P=0.911$). Conversely, independent *t*-test showed a significant difference in %s.d. of Cre between ASD individuals and TD subjects ($P=0.047$).

The multivariate analyses of covariances controlling the effect of structural differences between the ASD and TD subjects showed that the medial prefrontal NAA level was significantly higher in the ASD individuals than in the TD subjects ($F=4.832$, $P=0.033$). Moreover, the statistical conclusions did not change when the mixed- and/or left-handed subjects were excluded from the analysis. No significant difference was found in the other metabolite measures (Table 2).

Diagnostic differences in the relationships between age and NAA levels. A significant negative correlation between age and NAA levels was demonstrated in the TD group ($r=-0.618$, $P=0.001$), whereas no significant correlation between these indices was shown in the ASD individuals ($r=0.258$, $P=0.223$). These correlations were significantly different between the ASD and TD groups ($Z=-3.23$, $P=0.001$), indicating that the typical relationship between NAA level and age was absent in the ASD individuals (Figure 2). Furthermore, these statistical conclusions were totally preserved when the mixed- and/or left-handed subjects were excluded from the analysis.

Correlations with clinical indices. No significant correlation between the NAA and the ADI-R scores was found in the

Table 1 Demographic characteristics of the participants

	Subjects with ASD (N = 24)		*TD controls (N = 25)*		T-*test*	
Variables	*Mean*	*s.d.*	*Mean*	*s.d.*	t-*Value*	P-*value*
Age (range) (years)	29.5 (20–44)	6.9	29.4 (20–41)	6.2	−0.10	0.923
Height (cm)	170.3	5.0	174.0	6.1	2.29	0.027
Body weight (kg)	67.6	13.2	67.6	10.5	0.00	0.999
SES[a]	2.8	1.1	1.6	0.5	−5.13	0.000
Parental-SES[a]	2.3	0.7	2.2	0.4	−1.08	0.284
Handedness: right/mixed/left	19/3/2		25/0/0		χ^2	0.032
IQ						
FIQ	104.2	11.6	108.5	7.5	1.53	0.134
VIQ	111.3	14.0				
PIQ	91.3	14.6				
HFA**/Asperger/PDD-NOS	24/1/0					
Autism Diagnostic Interview-Revised						
Social	15.0	5.9				
Communication	12.4	3.3				
Repetitive	4.7	2.3				
Autism spectrum quotient	39.0	5.2	15.2	5.0	−15.76	0.000
Gray matter volume within VOI	5.2	0.3	4.9	0.4	−2.87	0.006
White matter volume within VOI	0.6	0.3	0.6	0.3	−0.25	0.801
Cerebrospinal fluid within VOI	2.2	0.3	2.5	0.3	3.14	0.003

Abbreviations: ASD, autism spectrum disorder; FIQ, full IQ; HFA, high-functioning autism; IQ, intelligence quotient; PDD-NOS, pervasive developmental disorder not otherwise specified; PIQ, performance IQ; SES, socioeconomic status; TD, typical development; VIQ, verbal IQ; VOI, volume of interest.
[a]Socioeconomic status, assessed using the Hollingshead index. Higher scores indicate lower status.

Table 2 Metabolite concentrations of participants

	MANCOVAs			
Metabolites	*d.f.*	*Effect size (f)*	*F-value*	P-*value*
N-acetylaspartate	47	1.26	4.83	0.033
Creatine	47	0.71	0.33	0.570
Choline-containing compounds	47	0.73	0.39	0.534
Glutamine + glutamate	47	1.00	1.82	0.184
Myo-inositol	47	0.73	0.39	0.534

Abbreviations: MANCOVA, multivariate analyses of covariance;d.f., degrees of freedom.
*Statistically significant after Bonferroni correction.

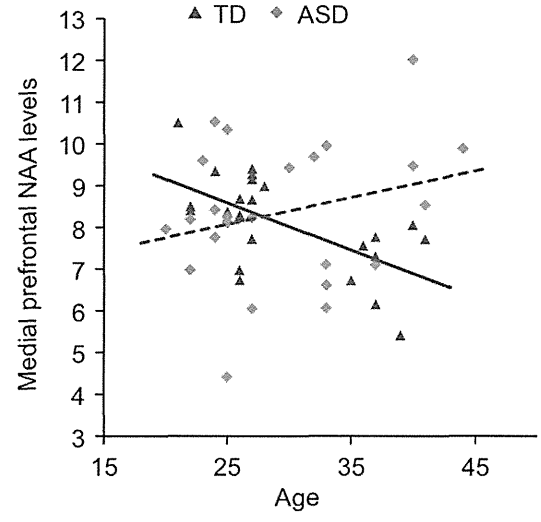

Figure 2 Relationships between age and *N*-acetylaspartate (NAA) level in the autism spectrum disorder (ASD) and typical development (TD) subjects. Scatter plots depicting correlations between frontal NAA levels and age of participants in individuals with ASDs and TD. The diagnostic difference of these correlations was statistically significant (Fisher's *r*-to-*z* transformation; $Z = -3.23$, $P = 0.001$).

ASD group. There was also no significant correlation between the NAA level and height, body weight, SES, parental-SES and IQ.

Discussion

The present study, utilizing 3-T ^{1}H-MRS, demonstrated significantly high medial prefrontal NAA in the non-medicated high-functioning adult males with ASDs compared with the demographically matched TD male subjects. Of note, while a significant negative correlation between age and medial prefrontal NAA levels was found in the TD group, such a correlation was absent in the ASD group. The difference in age–NAA relationships between the ASD and TD groups was reached at the statistically significant level.

The currently found atypical age-related NAA change in adult ASD subjects is in line with previous structural and functional imaging and post-mortem studies, which have reported different age-related trajectory in brain maturation between ASDs and TD during adulthood.[16,17,19,48–50] In particular, Murphy and his co-researchers, by their well-designed sequential studies, have repeatedly demonstrated an atypical relationship between age and brain structure, such as whole-brain GM volume,[49] cortical volume and cortical thickness (CT),[17] hippocampus volume[50] and streamline measured by diffusion tensor imaging,[19] in adolescence and

adults with ASDs compared with TD. Regarding functional aspects of brain aging, a functional MRI study demonstrated that brain activity during face processing task augments with age in adults with ASDs, but it decreases with age in TDs, and that the age-related increase in activity was correlated with changes in gaze behavior and improvements in social functioning.[18] One post-mortem study demonstrated atypical age-related change of microglial density both in GM and WM regions of brains in subjects with ASDs compared with TD.[48] Thus, there are accumulated evidences that have demonstrated atypical brain structural and functional age-related changes in individuals with ASDs during adulthood, which might underlie well-established age-related autistic symptom changes beyond childhood.[51–55] The current study further added new evidence that showed absence of age-related frontal NAA decline in people with ASDs during adulthood.

Although what NAA reflects is an area of debate, one possible explanation for the current findings is based on the notion that NAA, at least partially, reflects structural aspects such as neuron density or volume.[56] As hippocampal NAA reduction was reported to be correlated with volume reduction in adults with TD,[57] the current findings that NAA was negatively correlated with age in TDs, but not in ASDs, are partially concordant with a previous study that reported significant age-related frontal cortical volume and cortical thickness reduction in TDs, and less such relationship in the ASD group.[17] However, another well-designed study reported that CT in the temporal and parietal lobes, but not in the frontal lobes, was negatively correlated with age in the ASD group but not in the TD group.[15] Thus, the presence or absence of age–CT relationship in diagnostic groups and regions of brain are controversial among the various studies.[15,17] One potential explanation for the discrepancy is the influence of differences in ranges of ages between the studies (that is, ages from 12 to 24 years; Wallace *et al.*[15] vs 10 to 60 years; Raznahan *et al.*[17]). Although there are compelling pieces of evidence that frontal and temporal lobes have a key role in abnormal brain growth trajectory in ASD,[16,58] abnormal enlargement and subsequent normalization of frontal and temporal lobes in ASDs were suggested to not occur simultaneously.[16,24,58] Thus, the two previous studies may yield inconsistent results because of the different age range of participants as well as different brain areas examined.

Based on the notion that NAA also reflects functional aspects of neuronal tissues, one potential interpretation for the relationship between age and NAA is the age-related change of mitochondrial function. As NAA is synthesized from aspartate and acetyl-coenzyme A in mitochondria of neurons, and inhibitors of the mitochondrial respiratory chain decrease NAA levels, NAA has also been recognized as a marker of mitochondrial activity.[59,60] A recent meta-analysis demonstrated that biomarkers of mitochondrial dysfunction, such as lactate, pyruvate, carnitine and ubiquinone, were significantly deviated in individuals with ASDs from those with TD, and that the values of some of these markers correlated with autistic symptom severity.[61] In addition, prevalence of mitochondrial disease was shown to be much higher in ASD (approximately 5%) than in TDs ($<0.01\%$).[61] Post-mortem studies have shown that mitochondrial respiratory chain activity was increased in brains of ASDs compared with TD, which may result in an increase of NAA).[62,63] Overall, this evidence supports the idea that mitochondrial dysfunction is associated with ASDs (reviewed in Rossignol and Frye).[61] The concept of aging in mitochondrial function in TD individuals is well established by previous studies.[64] Taken together, age-related NAA reduction in TD subjects can reflect age-related decline of mitochondrial function, and ASD individuals may show atypical age-related change in frontal NAA levels due to dysfunctional mitochondria.

The current results seem to be at least partially different from one previous ^{1}H-MRS study, which revealed age-related NAA reduction in the amygdala–hippocampus complex in children and adults with ASDs but not in TD.[37] The discrepancy in the findings between the previous and current studies can be explained by considering the difference in age range of the study participants. The previous study examined the relationship between age and NAA levels in the combined group consisting of child and adult subgroups.[37] Age-related NAA decrease in TD subjects was not found in their study participants including children and adults. Thus, the previous study successfully examined age–NAA relationship during a period from childhood to adulthood, but they did not address the age-related change of NAA during adulthood.

The current study also identified significantly high frontal NAA levels of ASD individuals compared with the TD controls, which is concordant with results from the previous ^{1}H-MRS studies that located VOIs in the similar location in adults with ASDs.[65,66] Increased NAA level can result from not only increased synthesis but also decreased metabolism of NAA.[67] As NAA is synthesized in the mitochondria of neurons, neurons have been recognized to contribute significantly to NAA levels. 'NAA trapping theory' also suggests that NAA may increase even with dysfunction of metabolism of astrocytes or oligodendrocytes,[67] as recent studies have revealed that both astrocytes and oligodendrocytes are also involved in metabolism of NAA.[68] For example, patients with Canavan's disease, which is caused by mutations in the gene that codes for the enzyme aspartoacylase, which is necessary for NAA metabolism, demonstrates increased NAA without increased neuron density.[69] In addition, one experimental study showed that intravenous ethanol infusion, which enhances the activity of acetylaspartylase, a glial enzyme that degrades NAA, dynamically decreases cortical NAA measured by ^{1}H-MRS.[70] Thus, both increased NAA synthesis (for example, increased mitochondrial function in neuron) and decreased NAA metabolism (for example, depressed function of glia cell) can increase NAA in adults with ASD.

Several limitations and methodological considerations could be noted in the current study. First, though the current study was able to address the relationship between age and NAA measure across age span of 24 years (from 20 to 44 years), which is too wide to conduct a longitudinal study, the current cross-sectional study design could not directly address the individual aging effect. Second, compared with previous cross-sectional studies (for example, from 10 to 60 years; Raznahan *et al.*[17] and O'Brien *et al.*[37]), the age range of the current study participants was relatively narrow; thus, the current findings might not be generalized beyond young adulthood. As the pathophysiology of ASDs can be varied among different life stages, confinement to young adulthood

in the current study participants increased homogeneity of the neural mechanisms underlying ASDs. However, future studies should examine different stages during adulthood. Third, although the single VOI model yields high S/N,[71] the current study with no control VOI could not conclude whether this atypical age-related change in NAA is specific to medial PFC or was general to other brain regions. Fourth, although recruiting only male subjects in the current study decreased the heterogeneity of study participants and increased the reliability of results, it is unclear whether typical age–NAA relationship in TD subjects or absent of such relationship in ASD people can be generalized to female subjects.

In conclusion, the present findings demonstrated an absence of typical age-related medial prefrontal NAA decrement in ASD individuals during adulthood. Such an atypical relationship between age and NAA levels might contribute to a significant NAA increase in the ASD subjects compared with the TD adults. Although future studies should examine potential localization of atypical age-related NAA change and longitudinal course of autistic NAA abnormality, the current study has provided a new suggestion with regard to a role of atypical age-related NAA changes in the pathophysiology of ASD.

Conflict of interest

The authors declare no conflict of interest.

Acknowledgements. This study was supported in part by CREST (Japan Science and Technology Agency), and was also supported by KAKENHI (22689034 to HY; 20591378 to NY), the 'Development of biomarker candidates for social behavior' project carried out under the Strategic Research Program for Brain Sciences by the MEXT and the Global Center of Excellence (COE) Program 'Comprehensive Center of Education and Research for Chemical Biology of the Diseases' (NY).

1. Amaral DG, Schumann CM, Nordahl CW. Neuroanatomy of autism. *Trends Neurosci* 2008; **31**: 137–145.
2. Redcay E, Courchesne E. When is the brain enlarged in autism? A meta-analysis of all brain size reports. *Biol Psychiatry* 2005; **58**: 1–9.
3. Nordahl CW, Lange N, Li DD, Barnett LA, Lee A, Buonocore MH *et al.* Brain enlargement is associated with regression in preschool-age boys with autism spectrum disorders. *Proc Natl Acad Sci USA* 2011; **108**: 20195–20200.
4. Wolff JJ, Gu H, Gerig G, Elison JT, Styner M, Gouttard S *et al.* Differences in white matter fiber tract development present from 6 to 24 months in infants with autism. *Am J Psychiatry* 2012; **169**: 589–600.
5. Carper RA, Moses P, Tigue ZD, Courchesne E. Cerebral lobes in autism: early hyperplasia and abnormal age effects. *NeuroImage* 2002; **16**: 1038–1051.
6. Carper RA, Courchesne E. Localized enlargement of the frontal cortex in early autism. *Biol Psychiatry* 2005; **57**: 126–133.
7. Aoki Y, Aoki A, Suwa H. Reduction of *N*-acetylaspartate in the medial prefrontal cortex correlated with symptom severity in obsessive-compulsive disorder: meta-analyses of ^{1}H-MRS studies. *Transl Psychiatry* 2012; **2**: e153.
8. Ridderinkhof KR, Ullsperger M, Crone EA, Nieuwenhuis S. The role of the medial frontal cortex in cognitive control. *Science* **306**: 443–447.
9. Castelli F, Frith C, Happé F, Frith U. Autism, Asperger syndrome and brain mechanisms for the attribution of mental states to animated shapes. *Brain* 2002; **125**: 1839–1849.
10. Dapretto M, Davies MS, Pfeifer JH, Scott AA, Sigman M, Bookheimer SY *et al.* Understanding emotions in others: mirror neuron dysfunction in children with autism spectrum disorders. *Nat Neurosci* 2006; **9**: 28–30.
11. Wang AT, Lee SS, Sigman M, Dapretto M. Neural basis of irony comprehension in children with autism: the role of prosody and context. *Brain* 2006; **129**: 932–943.
12. Watanabe T, Yahata N, Abe O, Kuwabara H, Inoue H, Takano Y *et al.* Diminished medial prefrontal activity behind autistic social judgments of incongruent information. *PLoS One* 2012; **7**: e39561.
13. Chiu PH, Kayali MA, Kishida KT, Tomlin D, Klinger LG, Klinger MR *et al.* Self responses along cingulate cortex reveal quantitative neural phenotype for high-functioning autism. *Neuron* 2008; **57**: 463–473.
14. Lombardo MV, Chakrabarti B, Bullmore ET, Sadek SA, Pasco G, Wheelwright SJ *et al.* Atypical neural self-representation in autism. *Brain* 2010; **133**: 611–624.
15. Wallace GL, Dankner N, Kenworthy L, Giedd JN, Martin A. Age-related temporal and parietal cortical thinning in autism spectrum disorders. *Brain* 2010; **133**: 3745–3754.
16. Courchesne E, Campbell K, Solso S. Brain growth across the life span in autism: age-specific changes in anatomical pathology. *Brain Res* 2011; **1380**: 138–145.
17. Raznahan A, Toro R, Daly E, Robertson D, Murphy C, Deeley Q *et al.* Cortical anatomy in autism spectrum disorder: an *in vivo* MRI study on the effect of age. *Cereb Cortex* 2010; **20**: 1332–1340.
18. Bastiaansen JA, Thioux M, Nanetti L, van der Gaag C, Ketelaars C, Minderaa R *et al.* Age-related increase in inferior frontal gyrus activity and social functioning in autism spectrum disorder. *Biol Psychiatry* 2011; **69**: 832–838.
19. Pugliese L, Catani M, Ameis S, Dell'Acqua F, Thiebaut de Schotten M, Murphy C *et al.* The anatomy of extended limbic pathways in Asperger syndrome: a preliminary diffusion tensor imaging tractography study. *NeuroImage* 2009; **47**: 427–434.
20. Esbensen AJ, Seltzer MM, Lam KSL, Bodfish JW. Age-related differences in restricted repetitive behaviors in autism spectrum disorders. *J Autism Dev Disord* 2009; **39**: 57–66.
21. Kato T, Inubushi T, Kato N. Magnetic resonance spectroscopy in affective disorders. *J Neuropsychiatry Clin Neurosci* 1998; **10**: 133–147.
22. Friedman S, Shaw D, Artru A, Richards T. Regional brain chemical alterations in young children with autism spectrum disorder. *Neurology* 2003; **60**: 100–107.
23. Page LA, Daly E, Schmitz N, Simmons A, Toal F, Deeley Q *et al. In vivo* ^{1}H-magnetic resonance spectroscopy study of amygdala–hippocampal and parietal regions in autism. *Am J Psychiatry* 2006; **163**: 2189–2192.
24. Aoki Y, Kasai K, Yamasue H. Age-related change in brain metabolite abnormalities in autism: a meta-analysis of proton magnetic resonance spectroscopy studies. *Transl Psychiatry* 2012; **2**: e69–12.
25. Wu WE, Gass A, Glodzik L, Babb JS, Hirsch J, Sollberger M *et al.* Whole brain *N*-acetylaspartate concentration is conserved throughout normal aging. *Neurobiol Aging* 2012; **33**: 2440–2447.
26. Moreno-Torres A, Pujol J, Soriano-Mas C, Deus J, Iranzo A, Santamaria J. Age-related metabolic changes in the upper brainstem tegmentum by MR spectroscopy. *Neurobiol Aging* 2005; **26**: 1051–1059.
27. Gruber S, Pinker K, Riederer F, Chmelík M, Stadlbauer A, Bittsanský M *et al.* Metabolic changes in the normal ageing brain: consistent findings from short and long echo time proton spectroscopy. *Eur J Radiol* 2008; **68**: 320–327.
28. Brooks JC, Roberts N, Kemp GJ, Gosney MA, Lye M, Whitehouse GH. A proton magnetic resonance spectroscopy study of age-related changes in frontal lobe metabolite concentrations. *Cereb Cortex* 2001; **11**: 598–605.
29. Raininko R, Mattsson P. Metabolite concentrations in supraventricular white matter from teenage to early old age: a short echo time ^{1}H magnetic resonance spectroscopy (MRS) study. *Acta Radiol* 2010; **51**: 309–315.
30. Haga KK, Khor YP, Farrall A, Wardlaw JM. A systematic review of brain metabolite changes, measured with ^{1}H magnetic resonance spectroscopy, in healthy aging. *Neurobiol Aging* 2009; **30**: 353–363.
31. Lord C, Rutter M, Le Couteur A. Autism diagnostic interview-revised: a revised version of a diagnostic interview for caregivers of individuals with possible pervasive developmental disorders. *J Autism Dev Disord* 1994; **24**: 659–685.
32. Tsuchiya KJ, Matsumoto K, Yagi A, Inada N, Kuroda M, Inokuchi E *et al.* Reliability and validity of the autism diagnostic interview-revised—Japanese version. *J Autism Dev Disord;* PMID: 22806002 (in press).
33. Schopler E, Reichler RJ, DeVellis RF, Daly K. Toward objective classification of childhood autism: Childhood autism rating scale (CARS). *J Autism Dev Disord* 1980; **10**: 91–103.
34. Saemundsen E, Magnússon P, Smári J, Sigurdardóttir S. Autism Diagnostic Interview-Revised and the Childhood Autism Rating Scale: convergence and discrepancy in diagnosing autism. *J Autism Dev Disord* 2003; **33**: 319–328.
35. Pilowsky T, Yirmiya N, Shulman C, Dover R. The autism diagnostic interview-revised and the childhood autism rating scale: differences between diagnostic systems and comparison between genders. *J Autism Dev Disord* 1998; **28**: 143–151.
36. Kleinhans NM, Schweinsburg BC, Cohen DN, Müller R-A, Courchesne E. *N*-acetyl aspartate in autism spectrum disorders: regional effects and relationship to fMRI activation. *Brain Res* 2007; **1162**: 85–97.
37. O'Brien FM, Page L, O'Gorman RL, Bolton P, Sharma A, Baird G *et al.* Maturation of limbic regions in Asperger syndrome: a preliminary study using proton magnetic resonance spectroscopy and structural magnetic resonance imaging. *Psychiatry Res* 2010; **184**: 77–85.
38. Oldfield RC. The assessment and analysis of handedness: the Edinburgh inventory. *Neuropsychologia* 1971; **9**: 97–113.
39. Wakabayashi A, Baron-Cohen S, Wheelwright S, Tojo Y. The autism-spectrum quotient (AQ) in Japan: a cross-cultural comparison. *J Autism Dev Disord* 2006; **36**: 263–270.
40. Baron-Cohen S, Wheelwright S, Skinner R, Martin J, Clubley E. The autism-spectrum quotient (AQ): evidence from Asperger syndrome/high-functioning autism, males and females, scientists and mathematicians. *J Autism Dev Disord* 2001; **31**: 5–17.

41. First M, Spitzer R, Gibbon M, Williams J. *Structured Clinical Interview for DSM-IV Axis I disorders-Clinician Version (SCID-CV).* American Psychiatric Press: Washington, DC, 1997.
42. Wechsler D. *Wechsler Adult Intelligence Scale-Revised.* Psychological Corporation: New York, 1981.
43. Hollingshead AB. *Two-Factor Index of Social Position,* 1957.
44. Yamasue H, Fukui T, Fukuda R, Yamada H, Yamasaki S, Kuroki N *et al.* ^{1}H-MR spectroscopy and gray matter volume of the anterior cingulate cortex in schizophrenia. *NeuroReport* 2002; **13**: 2133–2137.
45. Lutkenhoff ES, van Erp TG, Thomas MA, Therman S, Manninen M, Huttunen MO *et al.* Proton MRS in twin pairs discordant for schizophrenia. *Mol Psychiatry* 2010; **15**: 308–318.
46. Hendry J, DeVito T, Gelman N, Densmore M, Rajakumar N, Pavlosky W *et al.* White matter abnormalities in autism detected through transverse relaxation time imaging. *NeuroImage* 2006; **29**: 1049–1057.
47. Petropoulos H, Friedman SD, Shaw DWW, Artru AA, Dawson G, Dager SR. Gray matter abnormalities in autism spectrum disorder revealed by T2 relaxation. *Neurology* 2006; **67**: 632–636.
48. Morgan JT, Chana G, Pardo CA, Achim C, Semendeferi K, Buckwalter J *et al.* Microglial activation and increased microglial density observed in the dorsolateral prefrontal cortex in autism. *Biol Psychiatry* 2010; **68**: 368–376.
49. McAlonan GM, Daly E, Kumari V, Critchley HD, Van Amelsvoort T, Suckling J *et al.* Brain anatomy and sensorimotor gating in Asperger's syndrome. *Brain* 2002; **125**: 1594–1606.
50. Murphy CM, Deeley Q, Daly EM, Ecker C, O'Brien FM, Hallahan B *et al.* Anatomy and aging of the amygdala and hippocampus in autism spectrum disorder: an *in vivo* magnetic resonance imaging study of Asperger syndrome. *Autism Res* 2012; **5**: 3–12.
51. Piven J, Harper J, Palmer P, Arndt S. Course of behavioral change in autism: a retrospective study of high-IQ adolescents and adults. *J Am Acad Child Adolesc Psychiatry* 1996; **35**: 523–529.
52. Seltzer MM, Krauss MW, Shattuck PT, Orsmond G, Swe A, Lord C. The symptoms of autism spectrum disorders in adolescence and adulthood. *J Autism Dev Disord* 2003; **33**: 565–581.
53. Shattuck PT, Seltzer MM, Greenberg JS, Orsmond GI, Bolt D, Kring S *et al.* Change in autism symptoms and maladaptive behaviors in adolescents and adults with an autism spectrum disorder. *J Autism Dev Disord* 2006; **37**: 1735–1747.
54. Farley MA, McMahon WM, Fombonne E, Jenson WR, Miller J, Gardner M *et al.* Twenty-year outcome for individuals with autism and average or near-average cognitive abilities. *Autism Res* 2009; **2**: 109–118.
55. Piven J, Bailey J, Ranson BJ, Arndt SN. An MRI study of the corpus callosum in autism. *Am J Psychiatry* 1997; **154**: 1051–1056.
56. Clarke CE, Lowry M, Horsman A. Unchanged basal ganglia *N*-acetylaspartate and glutamate in idiopathic Parkinson's disease measured by proton magnetic resonance spectroscopy. *Mov Disord* 1997; **12**: 297–301.
57. Schuff N, Amend DL, Knowlton R, Norman D, Fein G, Weiner MW. Age-related metabolite changes and volume loss in the hippocampus by magnetic resonance spectroscopy and imaging. *Neurobiol Aging* 1999; **20**: 279–285.
58. Courchesne E, Pierce K, Schumann CM, Redcay E, Buckwalter JA, Kennedy DP *et al.* Mapping early brain development in autism. *Neuron* 2007; **56**: 399–413.
59. Bates TE, Strangward M, Keelan J, Davey GP, Munro PM, Clark JB. Inhibition of *N*-acetylaspartate production: implications for ^{1}H MRS studies *in vivo*. *NeuroReport* 1996; **7**: 1397–1400.
60. Manji H, Kato T, Di Prospero NA, Ness S, Beal MF, Krams M *et al.* Impaired mitochondrial function in psychiatric disorders. *Nat Rev Neurosci* 2012; **13**: 293–307.
61. Rossignol DA, Frye RE. Mitochondrial dysfunction in autism spectrum disorders: a systematic review and meta-analysis. *Mol Psychiatry* 2011; **17**: 290–314.
62. Palmieri L, Papaleo V, Porcelli V, Scarcia P, Gaita L, Sacco R *et al.* Altered calcium homeostasis in autism-spectrum disorders: evidence from biochemical and genetic studies of the mitochondrial aspartate/glutamate carrier AGC1. *Mol Psychiatry* 2010; **15**: 38–52.
63. Napolioni V, Persico AM, Porcelli V, Palmieri L. The mitochondrial aspartate/glutamate carrier AGC1 and calcium homeostasis: physiological links and abnormalities in autism. *Mol Neurobiol* 2011; **44**: 83–92.
64. Green DR, Galluzzi L, Kroemer G. Mitochondria and the autophagy–inflammation–cell death axis in organismal aging. *Science* 2011; **333**: 1109–1112.
65. Murphy DGM, Critchley HD, Schmitz N, McAlonan G, Van Amelsvoort T, Robertson D *et al.* Asperger syndrome: a proton magnetic resonance spectroscopy study of brain. *Arch Gen Psychiatry* 2002; **59**: 885–891.
66. Oner O, Devrimci-Ozguven H, Oktem F, Yagmurlu B, Baskak B, Munir KM. Proton MR spectroscopy: higher right anterior cingulate *N*-acetylaspartate/choline ratio in Asperger syndrome compared with healthy controls. *Am J Neuroradiol* 2007; **28**: 1494–1498.
67. Moffett JR, Ross B, Arun P, Madhavarao CN, Namboodiri AMA. *N*-acetylaspartate in the CNS: from neurodiagnostics to neurobiology. *Prog Neurobiol* 2007; **81**: 89–131.
68. Baslow MH. Evidence that the tri-cellular metabolism of *N*-acetylaspartate functions as the brain's 'operating system': how NAA metabolism supports meaningful intercellular frequency-encoded communications. *Amino Acids* 2010; **39**: 1139–1145.
69. Janson CG, McPhee SWJ, Francis J, Shera D, Assadi M, Freese A *et al.* Natural history of Canavan disease revealed by proton magnetic resonance spectroscopy (^{1}H-MRS) and diffusion-weighted MRI. *Neuropediatrics* 2006; **37**: 209–221.
70. Gomez R, Behar KL, Watzl J, Weinzimer SA, Gulanski B, Sanacora G *et al.* Intravenous ethanol infusion decreases human cortical γ-aminobutyric acid and *N*-acetylaspartate as measured with proton magnetic resonance spectroscopy at 4 tesla. *Biol Psychiatry* 2012; **71**: 239–246.
71. Qayyum A. MR spectroscopy of the liver: principles and clinical applications. *Radiographics* 2009; **29**: 1653–1664.

OPEN ACCESS Freely available online PLoS one

Diminished Medial Prefrontal Activity behind Autistic Social Judgments of Incongruent Information

Takamitsu Watanabe[1], Noriaki Yahata[2,5], Osamu Abe[4,6], Hitoshi Kuwabara[3], Hideyuki Inoue[2], Yosuke Takano[2], Norichika Iwashiro[2], Tatsunobu Natsubori[2], Yuta Aoki[2], Hidemasa Takao[4], Hiroki Sasaki[4], Wataru Gonoi[4], Mizuho Murakami[4], Masaki Katsura[4], Akira Kunimatsu[4], Yuki Kawakubo[3], Hideo Matsuzaki[7], Kenji J Tsuchiya[8], Nobumasa Kato[7,9], Yukiko Kano[3], Yasushi Miyashita[1], Kiyoto Kasai[2,5], Hidenori Yamasue[2,7,9]*

1 Department of Physiology, The University of Tokyo, Bunkyo-ku, Tokyo, Japan, **2** Department of Neuropsychiatry, The University of Tokyo, Bunkyo-ku, Tokyo, Japan, **3** Department of Child Neuropsychiatry, The University of Tokyo, Bunkyo-ku, Tokyo, Japan, **4** Department of Radiology, Graduate School of Medicine, The University of Tokyo, Bunkyo-ku, Tokyo, Japan, **5** Global Center of Excellence (COE) Program, The University of Tokyo, Bunkyo-ku, Tokyo, Japan, **6** Department of Radiology, Nihon University School of Medicine, Itabashi-ku, Tokyo, Japan, **7** Japan Science and Technology Agency, CREST, Chiyoda-ku, Tokyo, Japan, **8** Osaka-Hamamatsu Joint Research Center for Child Mental Development, Hamamatsu University School of Medicine, Hamamatsu, Japan, **9** Department of Neuropsychiatry, Showa University School of Medicine, Tokyo, Japan

Abstract

Individuals with autism spectrum disorders (ASD) tend to make inadequate social judgments, particularly when the nonverbal and verbal emotional expressions of other people are incongruent. Although previous behavioral studies have suggested that ASD individuals have difficulty in using nonverbal cues when presented with incongruent verbal-nonverbal information, the neural mechanisms underlying this symptom of ASD remain unclear. In the present functional magnetic resonance imaging study, we compared brain activity in 15 non-medicated adult males with high-functioning ASD to that of 17 age-, parental-background-, socioeconomic-, and intelligence-quotient-matched typically-developed (TD) male participants. Brain activity was measured while each participant made friend or foe judgments of realistic movies in which professional actors spoke with conflicting nonverbal facial expressions and voice prosody. We found that the ASD group made significantly less judgments primarily based on the nonverbal information than the TD group, and they exhibited significantly less brain activity in the right inferior frontal gyrus, bilateral anterior insula, anterior cingulate cortex/ventral medial prefrontal cortex (ACC/vmPFC), and dorsal medial prefrontal cortex (dmPFC) than the TD group. Among these five regions, the ACC/vmPFC and dmPFC were most involved in nonverbal-information-biased judgments in the TD group. Furthermore, the degree of decrease of the brain activity in these two brain regions predicted the severity of autistic communication deficits. The findings indicate that diminished activity in the ACC/vmPFC and dmPFC underlies the impaired abilities of individuals with ASD to use nonverbal content when making judgments regarding other people based on incongruent social information.

Citation: Watanabe T, Yahata N, Abe O, Kuwabara H, Inoue H, et al. (2012) Diminished Medial Prefrontal Activity behind Autistic Social Judgments of Incongruent Information. PLoS ONE 7(6): e39561. doi:10.1371/journal.pone.0039561

Editor: Michelle Hampson, Yale University, United States of America

Received January 18, 2012; **Accepted** May 21, 2012; **Published** June 22, 2012

Funding: Part of this study was a result of the "Development of biomarker candidates for social behavior" project carried out under the Strategic Research Program for Brain Sciences by the Ministry of Education, Culture, Sports, Science and Technology, and was also supported by Grants-in-Aid for Scientific Research (22689034 to HY; 20591378 to NY), the Global Centre of Excellence (COE) Program "Comprehensive Centre of Education and Research for Chemical Biology of the Diseases" (NY) and a grant from the Japan Society for the Promotion of Science Research Foundation for Young Scientists (222882) to TW. The funders had no role in study design, data collection and analysis, decision to publish, or preparation of the manuscript.

Competing Interests: The authors have declared that no competing interests exist.

* E-mail: yamasue-tky@umin.ac.jp

Introduction

Individuals with autism spectrum disorders (ASD) have difficulties in processing of both verbal and nonverbal information [1–8]. Previous studies have demonstrated that they frequently underutilize verbally-supplied knowledge about other people, such as regarding their backgrounds and gender [5,9,10]. Other studies have revealed that they often inappropriately process nonverbal social information including facial expressions, voice prosody, and eye gaze [2,3,6,11–14]. Consequently, individuals with ASD often experience difficulty in interpreting complex social information, particularly when the verbal and nonverbal contents conflict with one another, which partially causes their frequent misinterpretation of irony and humor in real-life situations [9,15,16].

The characteristic behavioral responses to incongruent verbal-nonverbal information of ASD individuals have been reported in a previous study [17]. Compared with typically developed (TD) individuals, ASD individuals showed less sensitivity to the nonverbal content in incongruent information, even when they could effectively evaluate the verbal and nonverbal contents in isolation. This report is consistent with other behavioral studies that demonstrated that there are greater differences in the ability to process nonverbal information between ASD and TD individuals than in the ability to process verbal information

[18,19]. Although these observations imply that there are specific neural deficits that underlie this characteristic behavior in ASD individuals, to the best of our knowledge, no previous study has directly examined the neural deficits in ASD individuals that mediate their reduced use of nonverbal content when processing incongruent verbal-nonverbal social information.

Autistic responses to other types of incongruity have been investigated in a series of previous studies [4,5,7,20,21]. Previous neuroimaging studies revealed a neural mechanism underlying autistic responses to incongruity between *a priori* language-based knowledge and novel language-based information [5,7,21]. One of the studies revealed that the ventromedial prefrontal cortex in ASD individuals, compared with that in TD, did not show significant responses to pragmatic incongruity [5]. Another study demonstrated that activity in the left inferior frontal cortex is reduced in people with ASD during the integration of semantic social information [7]. Other neuroimaging studies examined neural response in individuals with ASD to incongruity between different types of nonverbal information (e.g., facial expression vs. voice prosody) [20] or their responses to stories provided as several sentences [4]. A study using cartoons revealed that the medial prefrontal and superior temporal regions in ASD subjects showed decreased activity during the presentation of ironic content [20]. Despite these findings on the neural basis of social incongruity processing in ASD individuals, little is known about the neural mechanisms underlying the characteristic autistic behavioral response to incongruity between verbal and nonverbal information.

In the present functional magnetic resonance imaging (fMRI) study, therefore, we aimed to reveal the neural mechanism underlying the imbalance between the interpretation of incongruent verbal-nonverbal social information in ASD individuals using realistic movie stimuli. In each of the short movie stimuli, a different professional actor spoke a word that was related to a positive or negative emotion while producing a positive or negative emotion-related facial expression and voice prosody (Fig. 1A). To directly investigate the neural response to this verbal-nonverbal incongruity, we did not give the participants any background knowledge or contextual information about the actors in the movies before conducting the fMRI scanning. Furthermore, we used a naturalistic psychological task wherein the participants responded as spontaneously as they do in real-life situations, because a previous behavioral study showed that autistic behavioral patterns are likely to be expressed in such spontaneous and automatic responses to social stimuli [19]. In the present study, the participants were instructed to judge an actor shown in a movie as a friend or a foe without explicit instruction about the incongruity itself, because the processing of incongruent social information occurs automatically in real-life situations, even when the subject does not explicitly attend to the incongruity (i.e., the Stroop effect has negligible influence) [22]. We analyzed the data according to the type of information that primarily affected the friend or foe judgments, and the judgments of the incongruent stimuli were classified into nonverbal-cue-biased or verbal-cue-biased judgments.

Based on previous behavioral findings [17–19], we hypothesized that the participants with high-functioning ASD would place disproportionately less emphasis on nonverbal content and make less frequent nonverbal-cue-biased judgments than TD participants. Hence, we assumed that the most characteristic impaired neural response in ASD individuals would be a difference in brain activity between verbal- and nonverbal-cue-biased judgments. To test this hypothesis, we compared the brain activity during

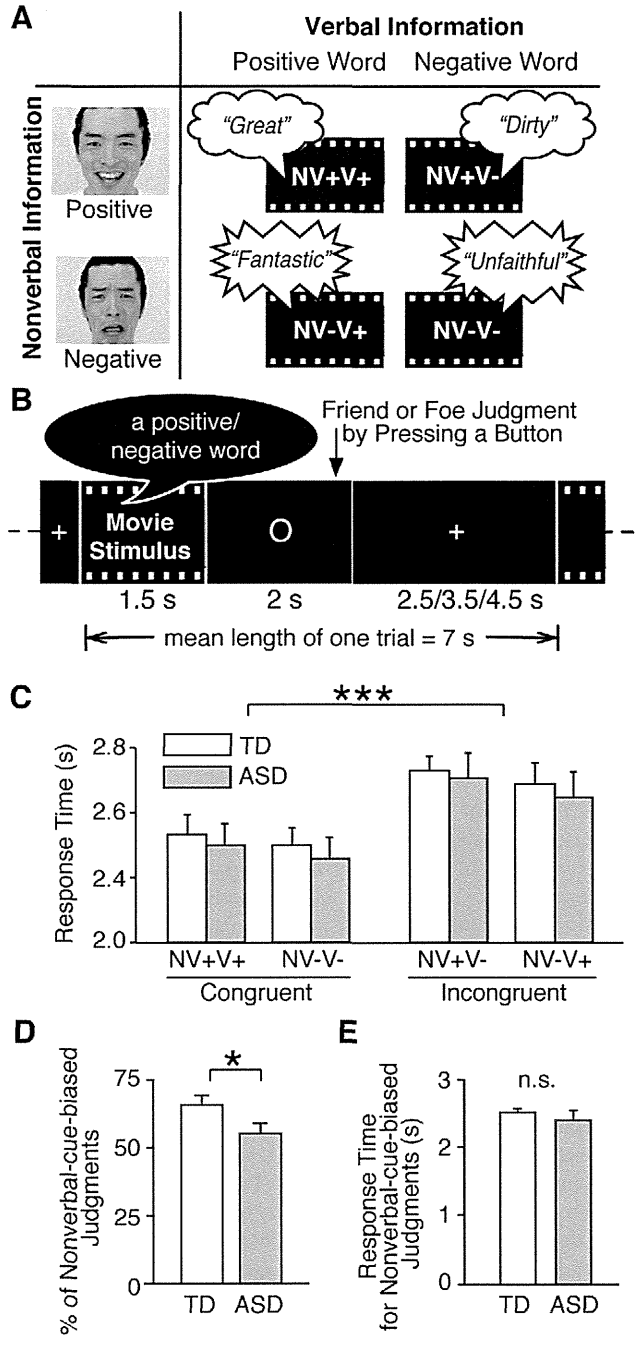

Figure 1. Task design and behavioral results. (A) Short movie stimuli. Our stimuli were short movies in which different professional actors spoke different emotional words (verbal information; positive and negative) while displaying different emotional facial expressions and voice prosody (nonverbal information; positive and negative). The emotional valence of the facial expressions was always the same as that of the voice prosody. Overall, the stimuli consisted of two types of congruent short movies (NV+V+: positive nonverbal and positive verbal information; NV-V-: negative nonverbal and negative verbal information) and two types of incongruent ones (NV+V-: positive nonverbal and negative verbal information; NV-V+: negative nonverbal and positive verbal information). **(B) Task design.** One trial of fMRI scanning session consisted of a 1.5 sec movie stimulus period, 2 sec response period, and a 2.5,3.5, or 4.5 sec fixation period. Participants were instructed to judge the person in each movie as friend or foe by pressing the corresponding buttons. **(C) Response times.** In a repeated-measure mixed-design two-way ANOVA, there was no

significant main effect of group (TD versus ASD) on response time, whereas there was a significant main effect of stimulus type (congruent versus incongruent). Response times for the incongruent stimuli were significantly longer than that for the congruent stimuli (***: $P<0.001$). To present the data, we further divided the stimulus types into more detailed categories. **(D) Number of nonverbal-cue-biased judgments.** ASD individuals exhibited significantly fewer nonverbal-cue-biased judgments of incongruent stimuli than the TD individuals (*: $P<0.05$) **(E) Response times for nonverbal-cue-biased judgments.** There was no significant difference in response time for nonverbal-cue-biased judgments of incongruent stimuli between the ASD and TD groups.
doi:10.1371/journal.pone.0039561.g001

nonverbal-cue-biased judgments in the ASD group with that in the TD group.

To focus on neural deficits mediating impaired social judgments in ASD individuals, we searched brain areas that are considered to be related to social judgments. Specifically, we estimated brain activity in anatomically-defined brain regions consisting of the medial prefrontal cortex (mPFC), precuneus, temporoparietal junction (TPJ), amygdala, superior temporal sulcus (STS), anterior insula (AI) and inferior frontal gyrus (IFG). According to several previous studies (see reviews in [23–25]), these regions are considered to underlie empathy processing, the mentalizing system, and uncertainty judgments, which are thought to be involved in social judgments.

Materials and Methods

Ethics Statement

The experiment protocol used in this study was approved by the ethics committee of The University of Tokyo Hospital (#1350). After a complete explanation of the study, written informed consent was obtained from all participants. Using longitudinal clinical assessments, a trained psychiatrist (H.Y.) confirmed that all of these adult participants had no intellectual disabilities, no need for psychotropic medication, and were capable of providing informed consent. Therefore, no participant needed someone else who consented on the behalf of the participants.

Participants

Fifteen male participants with ASD were recruited from the outpatient service of The University of Tokyo Hospital (Table 1). Fourteen were clinically diagnosed with high-functioning autism, while the remaining subject was diagnosed with pervasive developmental disorder-not otherwise specified. These diagnoses were based on the strict criteria of the Diagnostic and Statistical Manual-Revision IV [26], and they were conducted in consensus by two trained child-adolescent psychiatrists with more than ten years of clinical experience (H.Y. and N.K.) following more than two months of follow-up examinations. Another child adolescent psychiatrist (H.K.) confirmed the diagnoses of some patients using the Japanese version of the Autism Diagnostic Interview-Revised (ADI-R) [27]. For all participants who did not meet the threshold in the ADI-R social domain, the group was confirmed by the Childhood Autism Rating Scale (CARS) [28]. Previous studies have suggested that individuals classified as autistic according to both ADI-R and CARS had significantly lower IQ than those classified by CARS alone [29]. It is reasonable to suggest that the subsample of high-functioning ASD participants who did not meet ASD criteria based on ADIR, which is rated based on descriptive information by caregivers, could be classified with ASD based on CARS, which is rated by clinicians based on direct observations on behavior [30]. Thirteen of the 15 participants had never been prescribed psychotropic medication, whereas the other two has not taken medication for at least the previous seven months. The participants completed verbal and performance IQ tests, and they all exhibited estimated IQs ranging from average to above average. Seventeen healthy male TD participants were also recruited. All of the ASD and TD participants were interviewed by a trained psychiatrist (H.Y.) to screen for the presence of neuropsychiatric disorders using the Structured Clinical Interview for DSM-IV Axis I Disorder [31]. There were no significant differences in mean age, parental socioeconomic status (SES), handedness, or IQ between the ASD and TD groups.

The exclusion criteria for the both groups consisted of any history of current or past neurological illness, traumatic brain injury with any known cognitive consequences or loss of consciousness for more than five minutes, and substance abuse or addiction. An additional exclusion criterion for the TD group was a history of psychiatric disease or a family history of an axis I disorder among their first-degree relatives.

Details of the Questionnaires

Handedness was determined using the Edinburgh Handedness Inventory [32], and the participants with a laterality index of more than 0.5 were regarded as right-handed. The participants whose laterality index score ranged from −0.5 to 0.5 were defined as ambidextrous. The SES of the participants and their parents was assessed using the Hollingshead scale [33]. All participants completed a Japanese translation [34] of the 50-item Autism-Spectrum Quotient [35] within one month before or after the fMRI scanning. The IQ of the TD group was estimated using a Japanese version [36] of the National Adult Reading Test (NART) [37]. Although the NART can measure IQ accurately in TD participants, the test is problematic for ASD participants because of the well-known imbalances in their intellectual abilities. Therefore, the IQs of the ASD participants were assessed using the full scale of the Wechsler Adult Intelligence Scale Revised Japanese version [38]. Sleepiness during the MR scans was assessed using the Stanford Sleepiness Scale [39] and no participants fell asleep during the fMRI experiment.

MRI Scanning

A 3T MRI scanner (GE) was used in this experiment. The anatomical scanning sequence was a three-dimensional Fourier-transform spoiled-gradient-recalled acquisition during steady state (TR = 6.8 s, slice thickness = 1 mm, in-plane resolution = 1 × 1 mm). Gradient-echo echo-planar sequences were used for functional imaging (TR = 3 s, TE = 35 ms, flip angle = 80 degree, cubic voxel of 4 mm, 22 slices, from the ventral to dorsal slices). The first five functional images in each run were excluded from analysis to account for the equilibrium of longitudinal magnetization. Because the stimuli included human speech, we used an MRI-compatible headphone system (Hitachi, Corp. Tokyo, Japan), and confirmed before and after the experiment that the speech content and prosody in the stimuli could be heard clearly. A trained neuroradiologist (H.T. or O.A.) evaluated the MRI scans and found no gross abnormalities in any participant. Magnetic field inhomogeneities in our scanner were monitored with basic quality control conducted daily, and they were stable over the course of this study.

Task and Stimuli

The stimuli were 80 original monochrome movies with a length of 1,500 ms (see Supplementary materials). In each movie, one of 20 professional actors (10 male and 10 female) spoke a different emotional word accompanied by an emotional facial expression